LUMINESCENCE PROPERTIES OF RDX AND HMX

Paul L. Marinkas

Picatinny Arsenal
Dover, New Jersey

August 1975

TECHNICAL REPORT 4840

LUMINESCENCE PROPERTIES OF RDX AND HMX

PAUL L. MARINKAS

AUGUST 1975

PICATINNY ARSENAL
DOVER, NEW JERSEY

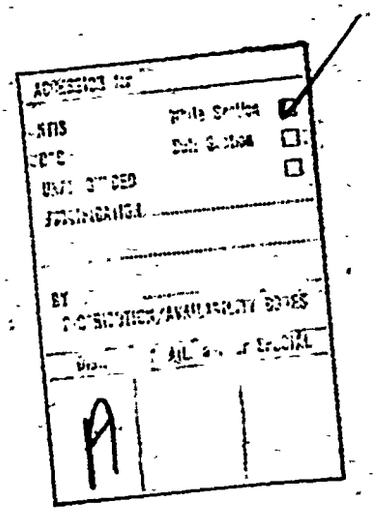

The findings in this report are not to be construed as an official Department of the Army Position.

DISPOSITION

Destroy this report when no longer needed. Do not return to the originator.

UNCLASSIFIED

SECURITY CLASSIFICATION OF THIS PAGE (When Data Entered)

REPORT DOCUMENTATION PAGE		READ INSTRUCTIONS BEFORE COMPLETING FORM
1. REPORT NUMBER Technical Report 4840	2. GOVT ACCESSION NO.	3. RECIPIENT'S CATALOG NUMBER
4. TITLE (and Subtitle) LUMINESCENCE PROPERTIES OF RDX AND HMX		5. TYPE OF REPORT & PERIOD COVERED 6. PERFORMING ORG. REPORT NUMBER
7. AUTHOR(s) Paul L. Marinkas		8. CONTRACT OR GRANT NUMBER(s) 1T161102AH5301
9. PERFORMING ORGANIZATION NAME AND ADDRESS Feltman Research Laboratory Picatinny Arsenal, Dover, NJ		10. PROGRAM ELEMENT, PROJECT, TASK AREA & WORK UNIT NUMBERS
11. CONTROLLING OFFICE NAME AND ADDRESS		12. REPORT DATE August 1975 13. NUMBER OF PAGES 93
14. MONITORING AGENCY NAME & ADDRESS(if different from Controlling Office)		15. SECURITY CLASS. (of this report) Unclassified 15a. DECLASSIFICATION/DOWNGRADING SCHEDULE

16. DISTRIBUTION STATEMENT (of this Report)

Approved for public release; distribution unlimited.

17. DISTRIBUTION STATEMENT (of the abstract entered in Block 20, if different from Report)

18. SUPPLEMENTARY NOTES

19. KEY WORDS (Continue on reverse side if necessary and identify by block number)

Band structure	Fluorescence	Optical absorption	Quantum yields
Charge transfer	HMX	Phosphorescence	Reflectance spectra
Circular dichroism	Lifetimes	Photodecomposition	RDX
Doping	Luminescence	Polynitramines	

20. ABSTRACT (Continue on reverse side if necessary and identify by block number)

Optical absorption measurements have confirmed the reports of earlier workers that the solid forms of the cyclic polynitramines known as RDX and HMX have a weak absorption band in the near ultraviolet which is not observed in spectra of the solvated compounds. Fluorescence measurements on solid samples of these materials show a weak emission, the excitation spectrum of which corresponds to this absorption band. The fluorescence is also not observed in the solvated

DD FORM 1 JAN 73 1473 EDITION OF 1 NOV 65 IS OBSOLETE

UNCLASSIFIED

SECURITY CLASSIFICATION OF THIS PAGE (When Data Entered)

20. Abstract (Continued)

compounds. Phosphorescence measurements on the solids reveal a long-lived emission, the excitation spectrum again corresponding to the band observed in absorption and fluorescence excitation. The lifetime of this emission was found to be substantially increased by deuteration. The absorption and luminescence bands are attributed to charge-transfer self-complexation in the solid state, and estimates of the charge-transfer singlet and triplet excited state energies are given.

The citation in this report of the names of commercial firms or commercially available products or services does not constitute official endorsement or approval of such commercial firms, products, or services by the U.S. Government.

ACKNOWLEDGMENT

The author wishes to express special thanks to Dr. N.E. Geacintov of New York University for his assistance in making the luminescence lifetime measurements, and for many helpful discussions. He wishes to also thank the Chief of the Solid State Branch of the Explosives Division, Dr. H.D. Fair, for encouraging this work, and the following members of the Division for their help: Mr. J. Leccacorvi, for supplying protonated HMX, Dr. S. Bulusu, for supplying deuterated RDX and HMX, and Mr. K. Edwards, for fabricating the luminescence spectrometer.

The work described herein was also submitted to the Faculty of the University of Delaware in partial fulfillment of the requirements for the degree of Doctor of Philosophy in Physics.

TABLE OF CONTENTS

INTRODUCTION

Review of Prior Literature

Luminescence spectroscopy of organic materials had its origin in the study of aromatic hydrocarbons such as anthracene or naphthalene. To this day the vast majority of work reported in the literature is concerned with this class of materials (Ref 1). Modifications to the basic aromatic structure, such as incorporation of a carbonyl (C = O) group, have provided variants which have received a great deal of study, an example being benzophenone. It is from the study of aromatic compounds and their variants that the basic principles of organic luminescence processes have been worked out.

Luminescence studies of nonaromatic compounds are very few, acetone being one example (Ref 2). The fluorescence and phosphorescence of acetone in rigid glass were studied at 77K and were found to consist of weak emissions with a good deal of overlap of the singlet and triplet emission spectra.

Physicists and chemists interested in the luminescence properties of explosive materials have generally preferred to study compounds which are basically aromatic, modified only by substitution of one or more nitro groups These compounds are usually difficult to purify, decompose easily, and are only weakly luminescent. McGlynn (Ref 3) has concluded that the effect of the nitro group is to reduce the fluorescence quantum efficiency by acting as a spin-orbit coupling center, thereby enhancing the intersystem crossing rate and reducing the lifetime of the triplet state. It is of interest to know to what extent these characteristics are maintained in going for aromatic to saturated nitro compounds. It has been generally assumed that, because aromatic nitro compounds are poor emitters of luminescence, the saturated compounds would also be nonemissive. This might have been true were it not for the appearance of a new phenomenon in the solid forms of the compounds described below.

The compounds 1,3,5 trinitro 1,3,5 triaza cyclohexane (RDX) and 1,3,5,7 tetranitro 1,2,5,7 tetraaza cyclooctane (HMX) are saturated heterocyclic (containing atoms other than carbon in the ring structure) compounds developed during World War II as explosives (the letters RDX stood for "Research Department Explosive"; HMX meant "High

Melting Explosive"). The nitro groups, which give these compounds their explosive character, are bonded to the ring nitrogen atoms (Fig 1). Since the resulting >N-NO_2 group is called a "nitramine" group, these compounds are sometimes referred to as "cyclic polynitramines".

The research program described in this dissertation had its beginnings as an exploratory effort into the possibility of detecting luminescent emission from RDX and HMX. This is a venture into a quite untravelled area of research, and the results were for many months negative. There existed only meager information on the optical absorption properties of these materials, particularly in the solid state. The literature contained no hint of any luminescences to be found in RDX or HMX, nor were any expected. In aromatic compounds the binding between molecules in the solid is weak, and for this reason it is of interest to study the properties of these tightly-bound solids for purposes of comparison. The luminescences described below in the cyclic polynitramines are believed to be a consequence of the type of bonding occurring in the solid.

The RDX molecule in solution is a nonplanar six-membered ring which exists in the so-called "chair" form (Fig 1). At ambient temperature the ring undergoes rapid interconversion in which the ring nitrogen atoms oscillate about the planar (sp^2) position (Ref 4). The molecular orbital calculations of Orloff, et al, indicate a relatively high positive charge ($q = +0.21$) on the carbon atoms and an even greater negative charge ($q = -0.33$) on the oxygen atoms (Ref 5).

The HMX molecule is based on an eight-membered ring; however the conformation of the ring in solution is not yet known. However, due to the strain expected in such a structure, the ring is almost certainly nonplanar in solution. No molecular orbital calculations have yet been performed on this molecule; however, since its optical absorption spectrum is almost identical to that of RDX, it seems reasonable to assume that conclusions drawn from the RDX calculations are applicable to HMX as well.

HMX is known to form molecular complexes with a variety of solvents (Ref 6) while RDX is known to complex with only two: sulfolane (Ref 7) and hexamethylphosphorus triamide (Ref 8).

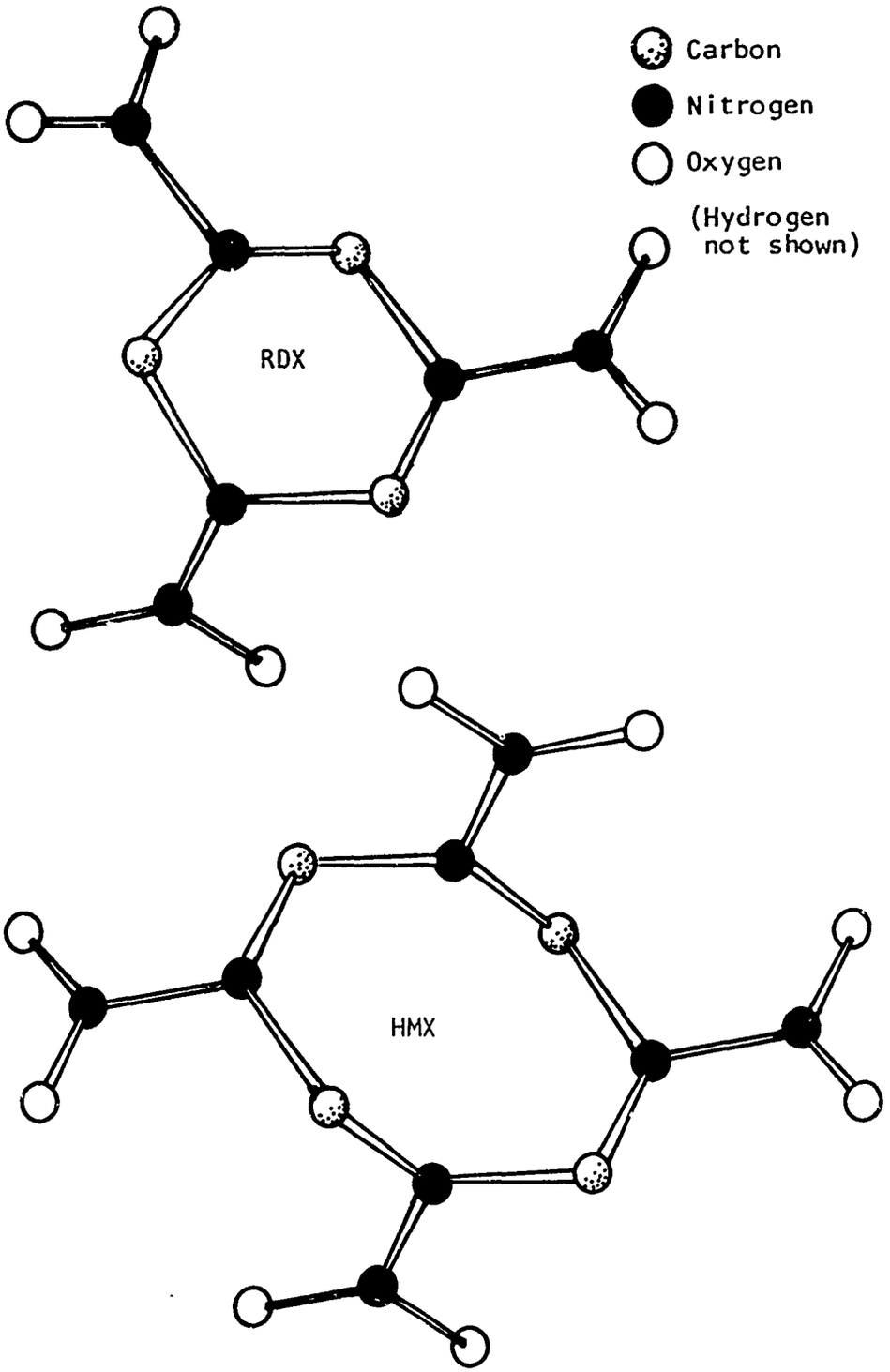

Fig 1 RDX and HMX molecules

Production quantities of RDX and HMX are prepared by the so-called "Bachmann process", which uses as raw materials hexamethylene tetramine ($(CH_2)_6N_4$), acetic anhydride, ammonium nitrate, and nitric acid. The parameters of the reaction can be adjusted to produce predominantly RDX or HMX, but the product is always a mixture of the two. Also produced are intermediates whose chemistry has been described by Bachmann and Sheehan (Ref 9) and by Wright, et al, (Ref 10). However, the HMX used in this work was not prepared by the Bachmann process, but by a new synthetic route developed by the Synthesis Group of the Explosives Division at Picatinny Arsenal, Dover, New Jersey. This process involves nitration of 1,5 diaceto 3,7 dinitro 1,3,5,7 tetraaza cyclooctane (or diaceto dinitro tetramine, or simply DADN). Since the starting reactant is an eight-membered ring compound, the product is not expected to contain any RDX impurity, which is based on a six-membered ring.

Although RDX and HMX are soluble enough in such solvents as acetone, nitromethane, or acetonitrile to permit purification by recrystallization and the growth of single crystals, they are practically insoluble in ethers, alcohols, and hydrocarbons. Those solvents which can dissolve appreciable quantities of these materials are either not transparent in the ultraviolet, have luminescences of their own, or do not form rigid glasses upon cooling. This has meant that it is not possible to study the isolated molecule in the standard glassy matrices such as EPA (a mixture of diethyl ether, isopentane, and ethyl alcohol). Therefore, it must be borne in mind that since powdered samples were studied in this work, some of the observed luminescence characteristics may have their origin in solid-state processes which may produce changes in excited state lifetimes, deviation of phosphorescence decay from exponential behavior, or spectral shifts.

The crystal structure of RDX has been the subject of a number of studies, the most recent being that of Choi and Prince (Ref 11). There are two known polymorphs, designated RDX (I) and RDX (II). The structure of RDX (II) has not been determined because of its instability. The stable form is orthorhombic, with eight molecules per unit cell. Orloff, et al, have remarked on the short C-O contact distance in crystalline RDX (Ref 5) and Stals (Ref 12) has concluded that the bonding in the crystal is dominated by electrostatic forces, rather than hydrogen or van der Waals bonding. Choi and Prince (Ref 11) also note several contact distances which are shorter than the sum of the van der Waals radii. The molecule is nonplanar in the crystal.

HMX can be crystallized in any of four polymorphic forms: the so-called α, β, γ and δ-forms. The first three all revert to the δ structure at elevated temperatures; β at 201°C, α at 203°C, and γ at 184°C (Ref 13). The temperature of the β-δ transition is lowered by approximately 15°C if the sample is irradiated with 254 nm ultraviolet light. Simultaneously, the ESR spectrum of a free radical identified by Stals (Ref 14) as NO_2 appears. Only the structures of the α-, the β-, and the δ-form are known. All forms have more than one molecule in a unit cell; Z = 8,2,4, and 6 for the α-, β-, γ-, and δ-forms. respectively. Stals (Ref 12) has noted the presence of short C-O distances similar to those observed in RDX, and in addition has pointed out a pairing of opposite sign net charges on the oxygen atoms (q = -0.35) and the nitrogen atoms (q = +0.76), although he does not make clear whether he is describing α- or β-HMX. Choi and Boutin (Ref 15), in the latest refinement of the β-HMX structure by neutron diffraction, conclude that all oxygen atoms on the periphery of the molecule are involved in contacts shorter than the sum of the van der Waals radii.

In summary, then, crystallographic investigations of RDX and HMX have shown the ability of these compounds to crystallize in various forms, and suggested that bonding in the solid is dominated by electrostatic forces. Molecular orbital calculations have revealed the existence of highly charged sites on the molecules, which could be the bonding sites between molecules in the solid. Such bonding could account for the high heats of sublimation for RDX (31.1 kcal/mol) and HMX (41.9 kcal/mol).

No luminescence studies of RDX and HMX have previously been reported. This is no doubt due to the fact that these materials in solution have their longest wavelength absorption band centered near 236 nm, (Ref 5) and it would have made sense for earlier workers to search for luminescence while irradiating in this band using solvated RDX and HMX. In fact, Stals (Ref 25) has reported making such a search with negative results. It will be a major conclusion of this report that the excited state of the isolated molecule which is populated by irradiation in the 236 nm band is dissociative rather than luminescent. The reason why luminescence occurs in the solid forms of these materials will be shown to be connected with the appearance of a new absorption band in the condensed phase. This band at 340 nm has been observed before (Ref 27,29), and has been considered to be a property of the solid, based on the fact that it is not observed in dilute solutions. However, it

is shown in the section entitled Characterization of Undoped RDX and HMX that the band is too weak to be seen using the low concentrations and short path length cells used to observe the much stronger absorption of the so-called "nitramine band" at 236 nm. New absorption measurements are described herein which make it clear that (1) there is indeed a new, weak absorption band in the solid that is absent in the spectra of the solvated material, and (2) this new band correlates well with the excitation spectra of fluorescence and phosphorescence emission from solid samples.

Even in the solid samples, the luminescences are very weak, and special techniques were necessary for their measurement. In order to maximize the exciting light flux, a powerful (1000 watt) xenon light source was coupled with a high aperture (f1.5) monochromator. A lock-in detection technique was used to extract the desired signal from the output of a high-sensitivity low-noise eleven-stage photomultiplier. The ultimate sensitivity was found to be limited only by background emissions.

Molecular Luminescence Theory

The luminescence properties of an isolated molecule can be understood from Figure 2, the so-called "Jablonski Diagram". The manifold of singlet states is shown on the left, and the triplet manifold on the right. Since the ground state is almost always a singlet, and since the optical selection rules forbid transitions between singlet and triplet states, the absorption spectrum of the isolated molecule is dominated by absorptions to higher singlet states. The lifetime of an excited state, be it singlet or triplet, is inversely related to the transition probability between that state and the ground state. A consequence of this fact is that the lowest excited singlet state has a radiative lifetime on the order of 10^{-8} seconds, while the lowest excited triplet can have a lifetime of the order of seconds, due to the forbidden nature of the transition.

For organic molecules, the term "fluorescence" is reserved for emission from the lowest singlet; the term "phosphorescence" is taken to mean emission from the lowest triplet to the ground state.

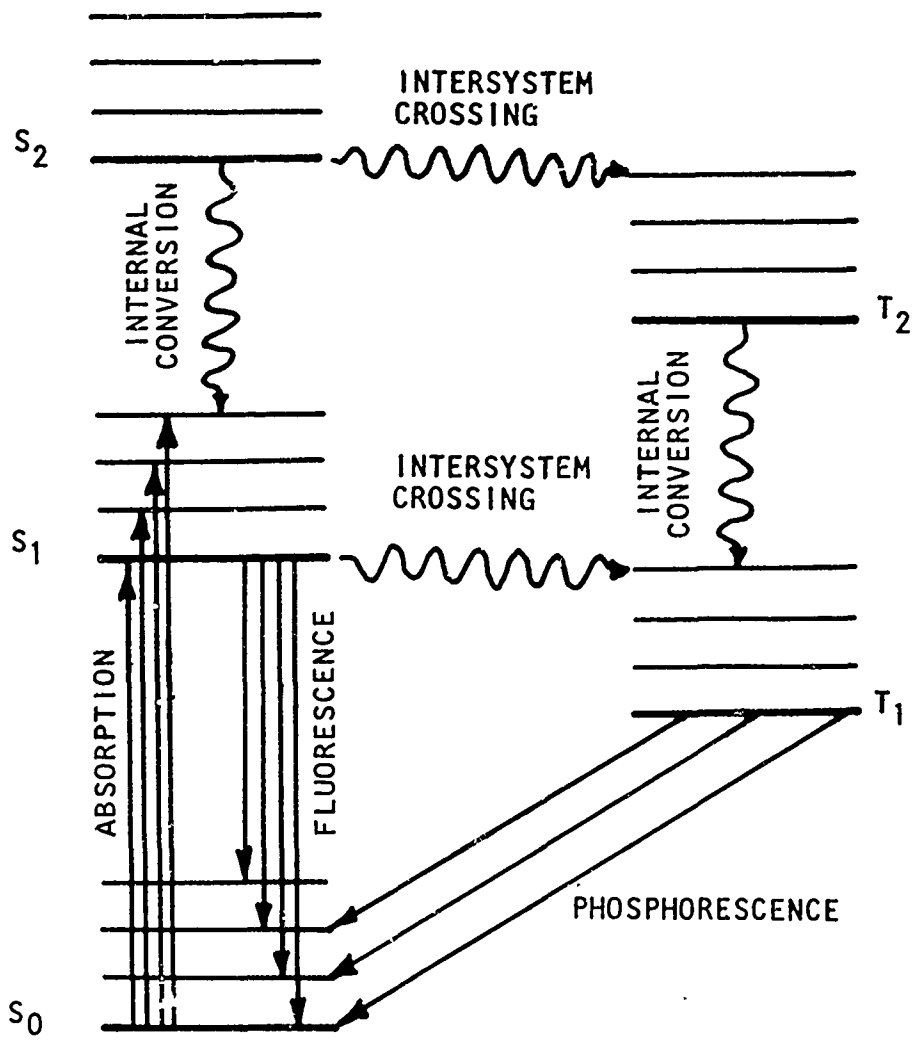

Fig 2 Energy level diagram for an isolated organic molecule

An excited molecule can spontaneously convert from a singlet to a triplet state by a process known as "intersystem crossing". This is a radiationless process which can occur because neither state is a pure singlet or triplet, due to the fact that spin-orbit coupling mixes a slight degree of singlet character into the triplet state, and vice versa. This process competes with radiative emission from the lowest singlet state, and if it is very efficient, fluorescence may be completely quenched. Spin-orbit coupling also renders the triplet-singlet transition more probable than its otherwise forbidden nature would indicate, and thus has a profound effect on the phosphorescence lifetime. Substitution of heavy atoms in a molecule shortens the phosphorescence lifetime (the "internal heavy-atom effect") because the heavy atoms act as spin-orbit coupling centers. The substitution of the nitro group is believed to have a similar effect (Ref 3).

The term "internal conversion" refers to a nonradiative transition between two states of the same multiplicity. Examples are conversions from higher singlet states to the lowest excited singlet, or even further down to the ground state. This is a basically similar process to intersystem crossing, except that, since it occurs between states of the same multiplicity, it is more probable by a factor of about 10^6. It is because this probability is so high that molecules excited to higher singlet or triplet states very soon find themselves in the lowest states of the same multiplicity, from which radiative transitions to the ground state ensue. This is the basis for "Kasha's rule", which states that fluorescence or phosphorescence originates from the lowest singlet or triplet state, respectively.

It is to be expected that the states of the isolated molecule will be altered when condensation to a crystal or some other aggregate such as a dimer or excimer occurs. New phenomena such as energy transfer can result, and absorption spectra can change.

The simplest possible aggregates are the dimer, a pair of identical molecules held together by weak interactions, and its excited counterpart, the excimer (the word excimer was coined as a combination of the words EXCIted diMER). In an excimer, there are then two equivalent sites for the excitation, and the transfer from one site to the other can be described as being due to simultaneous transitions, one upward and one downward, in the two molecules. The resonance of the excitation energy

between the sites has an effect on the excited state of the aggregate which is similar to the effect that the resonance of an electron between two nuclear centers has on the ground state of a molecule. That effect is to produce two resultant states for the aggregate, one stable with respect to separated molecules, and the other unstable. These states are analogous to the bonding and antibonding states of a diatomic molecule, which result from electron resonance. In the case of excitation resonance the splitting in energy of the two states is dependant on the relative orientation of the transition dipole moments of the two molecules, and on their separation. The relative orientation of the moments also determines whether transitions to the stable and unstable state are forbidden or allowed.

In an aggregate of N identical molecules the resonance interaction produces N-fold splitting of excited states spread into a band known as an exciton band. Only a few of these (equal in number to the number of molecules in a unit cell) can be reached by allowed electric dipole transitions. The forbidden exciton states, although not directly observable in an absorption experiment, play an important role in excitation and emission of molecular aggregates (Ref 16). A forbidden lowest exciton level in an exciton band corresponds to a metastable singlet level. If there is a lower-lying triplet, greatly enhanced intersystem crossing to the triplet level may result, leading to a greatly enhanced phosphorescence and quenching of the normal monomer fluorescence.

Excimers are by definition stable only in the excited state. If there exists a stable ground state, the pair of molecules is called a dimer. If the two molecules are not identical, the form stable in the ground state is called a complex; the form stable only in the excited state is called an exciplex (EXCIted comPLEX).

Excimer luminescence can be quite different from that of the monomer. For example, when pyrene is dissolved in high concentrations in a suitable solvent, a new fluorescence band is observed which is unstructured and at considerably longer wavelengths than the structured monomer fluorescence. Since the excimer does not form until one of the members of the pair has been excited, the excitation spectrum of the unstructured fluorescence is identical with the absorption spectrum of the monomer. Excimer formation can also occur in the solid phase, and excimer phosphorescence has also recently been reported (Ref 17).

Stevens (Ref 18) has studied excimer fluorescence in molecular crystals and has distinguished two types of lattice: the more common Type A, in which the overlap between neighboring molecules is small and/or the intermolecular spacing is relatively large; and Type B, in which adjacent molecules have a large overlap and are relatively closely spaced. The fluorescence emission of a Type A crystal is structured, and corresponds to the emission of the isolated molecule. The fluorescence spectrum of a Type B crystal is structureless, has a large Stokes shift, and is characteristic of the excimer. A Type A crystal can also display excimer fluorescence due to the presence of defects at which adjacent pairs of molecules are close enough to allow excimer formation. These sites then act as traps for energy carried by excitons, and excimer fluorescence appears, in addition to the normal monomer fluorescence. Microcrystalline films and crystals under high pressure have a high density of defects, and have been used to induce and study excimer fluorescence.

Dimers, in which the identical molecules are held together in the absence of excitation of either one, and complexes, which differ only in the fact that the members of the pair need not be identical, can be held together by various types of interactions. The anthracene photodimer (it is formed under excitation by light, but once formed, has a stable ground state) is held together by a chemical bond. Hydrogen-bonded complexes were already recognized in the 1930's. The water molecule can bond to others of the same type by charge-transfer forces (Ref 19). This latter type of bonding is the result of yet another type of resonance; that derived from mixing of a "dative" and a "no-bond" structure. The complex formed when two dissimilar molecules are held together by this type of force is sometimes referred to as a charge-transfer complex, or donor-acceptor (DA) complex. Mulliken (Ref 19) has represented the ground, or "normal" state of such a 1:1 complex in terms of the normal state wave functions ψ_D and ψ_A of the electron donor (D) and acceptor (A), with corrections to account for the interaction:

$$\psi_N = a\psi_0\ (D,A) + b\psi_1\ (D^+\text{-}A^-) \qquad (1)$$

The quantities a and b range from 0 to 1, and their relative magnitudes are indication of the degree of charge transfer in the ground state of the complex. Here the "no-bond" wave function ψ_0 is an antisymmetrized product of the functions ψ_D and ψ_A, corrected for effects such as polarization.

The "dative" wave function ψ_1 is of Heitler-London type for the hypothetical D-A pair obtained by removing one electron from a molecular orbital in D, putting it in a previously unoccupied orbital of A, and forming a bond between the odd electrons then available, one on D and one on A.

The excited state ψ_E of the complex is described by

$$\psi_E = a^* \psi_1 \ (D^+-A^-) - b^* \psi_0 \ (D,A) \qquad (2)$$

where, as a first approximation, $a^* = a$, $b^* = b$. Thus, excitation from ψ_N to ψ_E corresponds to transfer of charge from D to A. The complex as a whole is more stable than the separated D and A due to resonance stabilization from mixing of the dative and no-bond structures.

Whether a molecule functions as a donor or an acceptor in a complex depends a good deal on the partner. Aromatic molecules, for example anthracene, are notably amphoteric in this respect, acting as donors toward strong acceptors and as acceptors toward strong donors. In fact, many molecules can function simultaneously as donors and acceptors in complexes stabilized by two-way charge transfer. The same molecule may function as a donor at one site and as an acceptor at another (Ref 19).

The transition between ψ_N and ψ_E is usually intense, and leads to a new absorption band not characteristic of the isolated donor or acceptor. When a charge-transfer complex is excited in this band, the system exhibits two types of luminescence:

1. Fluorescence characteristic of the complex and corresponding to the $\psi_E \rightarrow \psi_N$ transistion, and

2. Phosphorescence, which may be characteristic of the donor, the acceptor, or the complex.

The charge-transfer complex fluorescence spectrum is a broad, structureless band, which occurs at an energy near that of the donor phosphorescence (Ref 20). The lifetime is characteristic of the complex, and is unrelated to that of the donor. The spectrum is nearly mirror-symmetric to the corresponding charge-transfer absorption band.

Excitation of the complex into its first excited singlet state leads, in addition to fluorescence, to intersystem crossing to the lowest excited triplet state of the complex, $^3(DA)^*$, followed by dissociation into either of the two locally-excited states $^3(D^*A)$ or $^3(DA^*)$, or, if the triplet state of the complex lies lower in energy than either of the locally excited triplet states, phosphorescence characteristic of the complex will occur. The most usual case is for the phosphorescence to resemble that of the donor. Since the two unpaired electrons in a typical charge-transfer complex occupy different orbitals which are more or less localized on the donor and acceptor, the singlet-triplet splitting will be small (Ref 21). Considerable overlap between the fluorescence and phosphorescence can thus be expected. Indeed, in several cases the spectra coincide; however, this is attributed to delayed emission which does not occur from the triplet state directly, but as fluorescence from the charge-transfer singlet state which is thermally populated from the triplet state (Ref 22).

Energy transfer from an excited (energy) donor molecule to a ground state acceptor is a general phenomenon, provided that the acceptor energy level is lower lying than the donor energy level. For example, triplet-triplet energy transfer was first clearly demonstrated by Terenin and Ermolaev (Ref 23) who excited the phosphorescence of the naphthalene acceptor by triplet transfer from a benzophenone donor in rigid solution at 77K. The energy E_{ex} of the exciting light and the singlet excitation energies E_D and E_A of the donor and acceptor molecules were chosen such that

$$E_A > E_{ex} > E_D. \qquad (3)$$

Thus, only the donor molecules were excited by the incident light. Intersystem crossing by

$$^1D^* \rightarrow {}^3D^* \qquad (4)$$

led to a triplet donor population, and since the donor triplet energy was larger than that of the acceptor, the transfer

$$^3D^* + {}^1A \rightarrow {}^3A^* + {}^1D \qquad (5)$$

was followed by acceptor phosphorescence. That the transfer was from the donor triplet state was assured by the fact that the donor singlet

state was lower in energy than that of the acceptor, and therefore transfer by

$$^1D^* + {}^1A \rightarrow {}^1A^* + {}^1D \qquad (6)$$

was forbidden by conservation of energy. That the acceptor state was the triplet was evident from the spectral and time dependance of the emission. The wavelength dependance of the excitation reproduced the absorption spectrum of the donor.

The singlet state energy of naphthalene is about 4eV, as deduced from the wavelength (310.5 nm) of the 0-0 transition measured in hexane solution. At longer wavelengths the compound is transparent. The triplet state energy as deduced from the wavelength (470 nm) of the 0-0 band of the phosphorescence in EPA glass at 77K is 2.64 eV. Thus, naphthalene can accept energy from a donor by triplet-triplet transfer provided the triplet state energy of that donor exceeds 2.64 eV. The naphthalene singlet state will not be excited directly if the wavelength of the exciting light is greater than about 310 nm.

Although the experiment of Terenin and Ermolaev was done in rigid glass solution, the same process can occur in the crystalline state. One way in which this can happen is if the host crystal acts as the energy donor, with an impurity molecule acting as the acceptor. Excitation into the host singlet exciton band is observed to give rise to guest phosphorescence by triplet-triplet transfer. Here, however, the periodicity of the host lattice has as one of its consequences the fact that excitation can migrate through the lattice in the form of excitons, mobile pseudo-particles of energy. Triplet excitons, by virtue of their long lifetime, can transport energy considerable distances from the site of the original excitation. If the exciton encounters an impurity molecule whose triplet energy level lies lower than the host triplet exciton band, the excitation will be transferred to the guest, and guest phosphorescence will result. The exciton is said to be "trapped" on the impurity, and is no longer mobile.

A more complicated system is one in which a host crystal is doped with two types of impurities. An example is the biphenyl (host)- phenanthrene-naphthalene (guests) system studied by Hirota and Hutchison (Ref 24), in which the molecular triplet energy levels of both phenanthrene and naphthalene lie slightly below the triplet exciton band of the biphenyl host.

These authors used ESR to study the decay rates of the guest triplet states. The temperature dependance of these rates provided an activation energy for transfer which corresponded to the spectroscopic energy difference between the triplet energy of phenanthrene and the triplet exciton energy of biphenyl. Thus, in this type of guest-guest transfer, thermal activation from guest donor triplet to host exciton band is necessary. If the energy gap is too large to be bridged by thermal energy, energy transfer via exciton motion cannot occur.

EXPERIMENTAL

Sample Preparation

RDX was prepared by the Bachmann process, and was fractionally recrystallized a minimum of five times from spectrograde acetone. HMX was prepared by nitrolysis of DADN, washed with hot water to remove linear nitramines, and recrystallized a minimum of five times from spectrograde acetone.

Luminescence Spectrometer

The luminescence spectrometer is built around a quartz cylinder which is rotated at high speed by an air turbine. The cylinder is painted black except for three clear windows 120° apart, and rotates between an inner and outer light baffle, each of which has two apertures at 90° to one another. One aperture admits light from the excitation monochromator, and the other allows phosphorescence emitted by the sample to enter the emission monochromator (Fig 3). When a window on the quartz cylinder is lined up with the excitation aperture, the sample is exposed to the exciting light. As the cylinder rotates, closing the excitation aperture, another window lines up with the emission aperture, allowing phosphorescence emission to enter the emission monochromator. Since the excitation and emission apertures are not open simultaneously, excitation light cannot reach the emission monochromator directly.

The phosphoroscope was equipped with filter drawers at the excitation and emission ports which could accommodate 2 x 2" glass filters, or polarizing films.

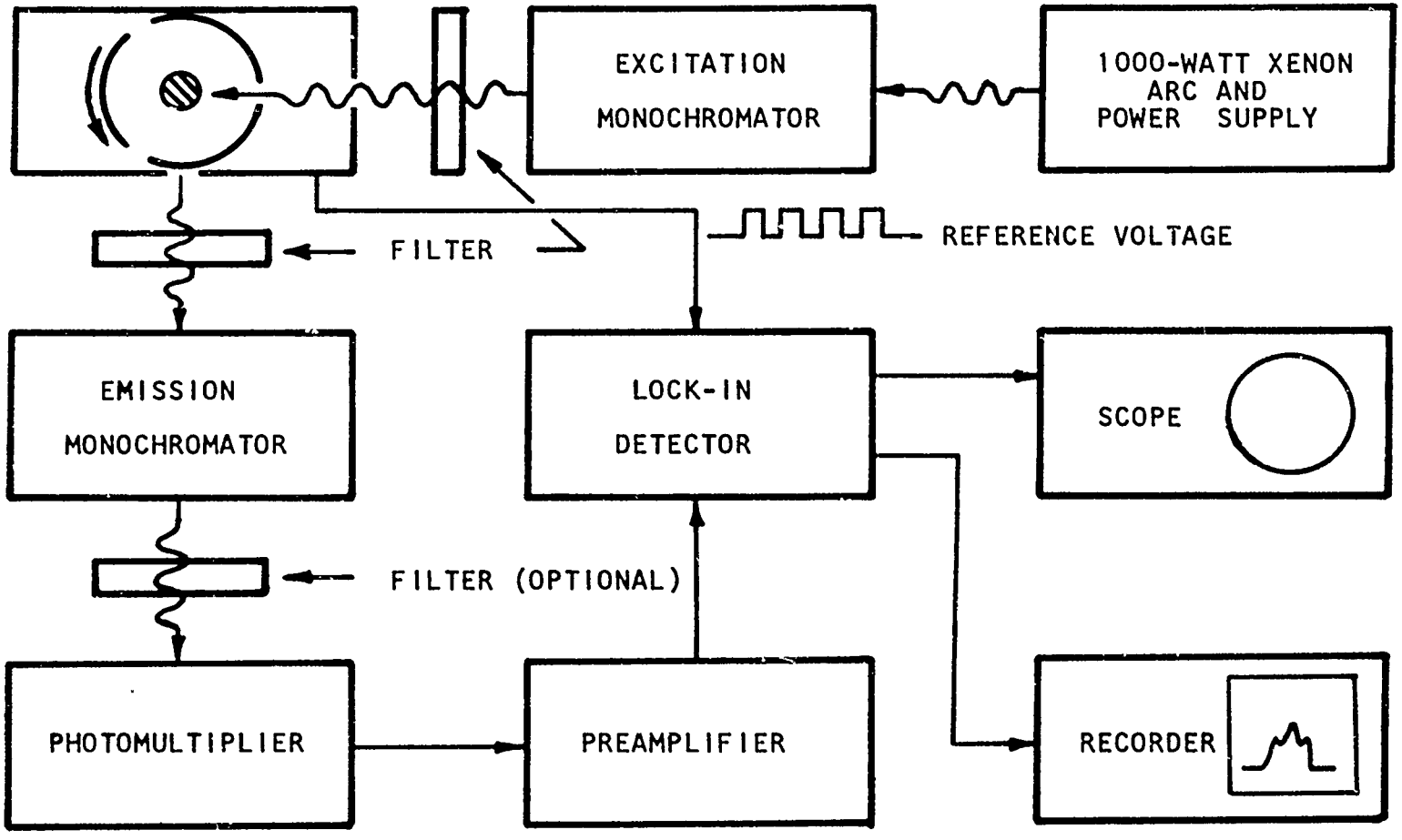

Fig 3 Luminescence spectrometer block diagram

For fluorescence measurements, the three-window shutter was replaced with a four-window type, which had windows at 90° to one another. With this arrangement, the sample was viewed while illuminated by the excitation monochromator. For measurement of weak fluorescences such as those exhibited by RDX, it was necessary to reduce the background fluorescence to a minimum, and for these measurements an Aminco Bowman Spectrofluorometer was employed.

Corresponding to the three (or four) windows which chopped the exciting and emitted light, the stem of the rotating shutter was equipped with an equal number of windows which, together with an infrared-emitting diode and a semiconductor light-activated switch, form a circuit for generating a square-wave reference voltage for the lock-in photometer. The infrared-emitting diode is isolated from the sample chamber by the baffling system, and emits at a wavelength (900 nm) to which the photomultiplier detector is insensitive.

The turbine which operates the cylindrical shutter is an NMR sample spinner powered by compressed nitrogen. The spent gas is led upward through the hollow stem of the shutter, where it bathes the tail of the liquid nitrogen or helium dewar containing the sample, in order to prevent the condensation of water vapor. The fact that there are no moving metallic parts allows the system to be used in a magnetic field, should this be desired.

Since very weak luminescences were expected from RDX and HMX, the light source chosen for excitation was a 1000-watt xenon arc followed by a large aperture (f1.5) monochromator manufactured by the Spectrolab Company. The monochromator could be scanned electrically over the range 120-1000 nm, and was followed by a Corning No. 7-54 glass filter inserted in the excitation filter drawer to absorb any second-order light.

Light emitted by the sample was passed through a quartz lens and focussed on the entrance slit of a second monochromator, a Gamma Scientific Model No. 700-31 grating instrument. This device could be electrically scanned in two ranges from 200 to 800 nm. When required, order-sorting filters were automatically inserted into the beam by the monochromator mechanism.

Light leaving the monochromator was incident on the photocathode (bialkali) of an 11-stage photomultiplier. Because of the bialkali photocathode, the tube did not require cooling to reduce the dark current to acceptable levels.

Signals from the photomultiplier were fed to a Pacific Photometric Model No. 62/3A27 preamplifier and current-to-voltage converter before being synchronously demodulated by a Pacific Photometric Model No. 350 lock-in photometer. This device combines the signal with the reference voltage generated by the phosphoroscope and generates a DC voltage proportional to the amplitude of the luminescence. This voltage was fed to the Y-axis of an X-Y recorder and plotted as a function of either excitation or emission wavelength.

Quartz or pyrex tubes 5 mm in diameter were used to hold the sample powders. For the weaker phosphorescer, HMX, the quartz tubes were found to contribute a background signal amounting to about 40% of the total. Thin-walled pyrex tubes were found to be less troublesome in this regard, but were not considered trustworthy for excitation wavelengths shorter than about 300 nm because of absorption in the glass. Fortunately, measurements with quartz tubes showed no sample excitation below about 320 nm, and so pyrex tubes were used whenever possible.

Lifetime Measurements

Phosphorescence lifetimes were measured with apparatus at the Department of Chemistry at New York University, a block diagram of which is shown in Figure 4. Following a 1 ms flash excitation from a photographic flash gun equipped with a Corning No. 7-60 glass filter, phosphorescence emitted by the sample was conducted through a fiber optic to a Corning No. 3-70 viewing filter and thence to the photomultiplier tube. The signal from the photomultiplier was preamplified, digitized, and fed to a digital signal averager. The decay curve was averaged over several flashes, and then printed out by teletype. The sample temperature in all the phosphorescence decay measurements was 77K.

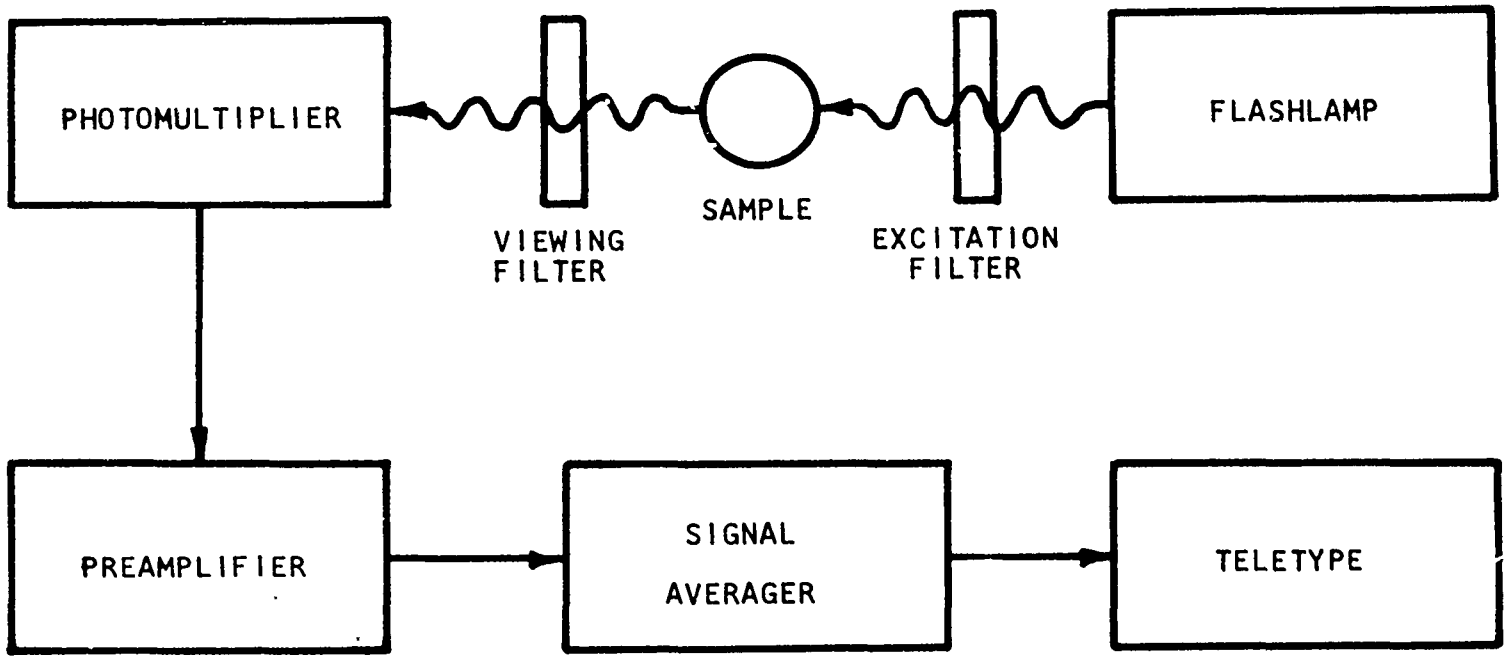

Fig 4 Apparatus for measurement of phosphorescence decay

Fluorescence decay curves were measured with a photon counting apparatus, again at New York University. A block diagram of the apparatus is shown in Figure 5. The flashlamp power supply fires the lamp and simultaneously delivers a "start" signal to the time-to-pulse height converter. The lamp output is filtered by a 340 nm interference filter with a 14 nm bandwidth at half-height. Sample fluorescence excited by this wavelength is filtered by Corning No. 3-73 glass filter, and is incident on the photomultiplier. A pulse-height discriminator discards all signals below the threshold signal corresponding to the reception of a single photon. The output from the discriminator is shaped and used as a "stop" signal for the time-to-pulse height converter.

In operation, the photomultiplier is stopped down until, on the average, one emitted photon is received for every ten excitation flashes. The time interval between the reception of the "start" signal and the "stop" signal is the time required for emission of a photon, and is converted to a pulse height and stored in the signal averager. The accumulated number of photons detected as a function of the time required for their emission is the averaged decay curve, which is printed out by the teletype.

The lifetimes for RDX and HMX were comparable to the decay time for the excitation from the lamp, which was a few nanoseconds. Therefore the measurement of an unknown was always preceded by establishing the "lamp profile" using an MgO nonfluorescent standard sample. The measurement temperature for all fluorescence decay curves was 300K.

The photon counting apparatus was also used to check for the presence of any short-lived phosphorescences. No shorter phosphorescence decay time than the ones reported in Table 1 were found.

CHARACTERIZATION OF UNDOPED RDX AND HMX

Reflectance Spectra of Single Crystals

The absorption spectrum of RDX in acetonitrile solution consists of two distinct bands at 236 nm ($\varepsilon = 11,000\ M^{-1}cm^{-1}$) and at 195.5 nm ($\varepsilon = 16,400\ M^{-1}cm^{-1}$) with weak vibrational structure superimposed on each band (Ref 5). Orloff, etal, assigned these absorptions primarily to $\pi \rightarrow \pi^*$ transitions localized on the NO_2 groups. In addition they concluded that there were weak $n \rightarrow \pi^*$ absorptions buried in the 236 nm band

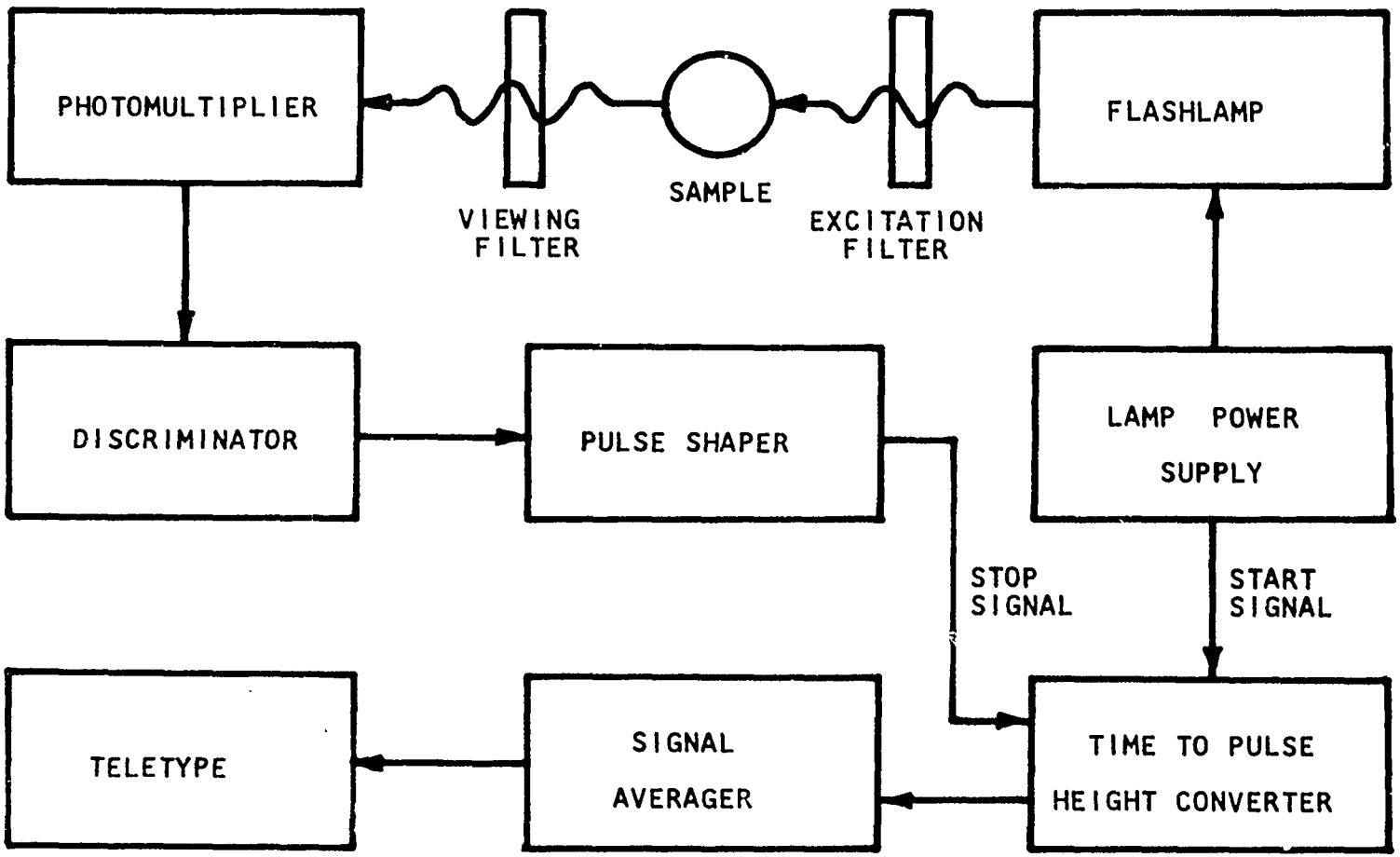

Fig 5 Apparatus for measurement of fluorescence decay

which result from the promotion of nonbonding electrons on the oxygen atoms. We will refer to this system of overlapping bands as the "nitramine band" since, as pointed out by Stals (Ref 25), the π, n, and σ orbitals are intimately mixed in nitramine type molecules. Orloff, et al, assigned the lowest excited state of RDX to an $n \rightarrow \pi^*$ transition occurring in the long wavelength tail of the nitramine band.

At this writing there are no molecular orbital calculations available for HMX, but since its absorption spectrum is essentially the same as that of RDX, it seems reasonable to assume that the above assignments apply.

A question of fundamental interest is the nature of the electronic transition by which the subject molecule is excited to the luminescent state. The fluorescence and phosphorescence excitation spectra of powdered RDX and HMX show excitation at wavelengths longer than those absorbed by the solvated compounds, and thus their absorptions at wavelengths in the region 320-420 nm in the solid state are of interest.

Absorption spectra derived from specular reflectance measurements (Ref 26) on RDX and HMX single crystals are shown in Figures 6 and 7, which show a weak, ill-defined band near 340 nm. Similar measurements by Stals (Ref 27) show a more distinct band. Based on the fact that this band is observed in the solid and (apparently) not in solution, Stals attributed it to charge-transfer self-complexation in the solid.

Since this weak absorption band appears superimposed on the tail of the nitramine band, we can make use of Urbach's rule to estimate its true shape. This rule predicts that the absorption tails of bands in certain solids follow the expression (Ref 46,47)

$$\varepsilon(\nu) = \text{Const}\ e^{-(\nu-\nu_0)/kT} \qquad (7)$$

where ν_0 is the frequency at which the molar absorptivity ε is maximum for the band in question. If the frequency interval is narrow, the expression can be rewritten in terms of wavelength

$$\varepsilon(\lambda) = A\ e^{-\Delta\lambda/B} \qquad (8)$$

where A and B are to be determined from the measured absorption spectrum, and $\Delta\lambda$ is the deviation in wavelength from the absorption peak.

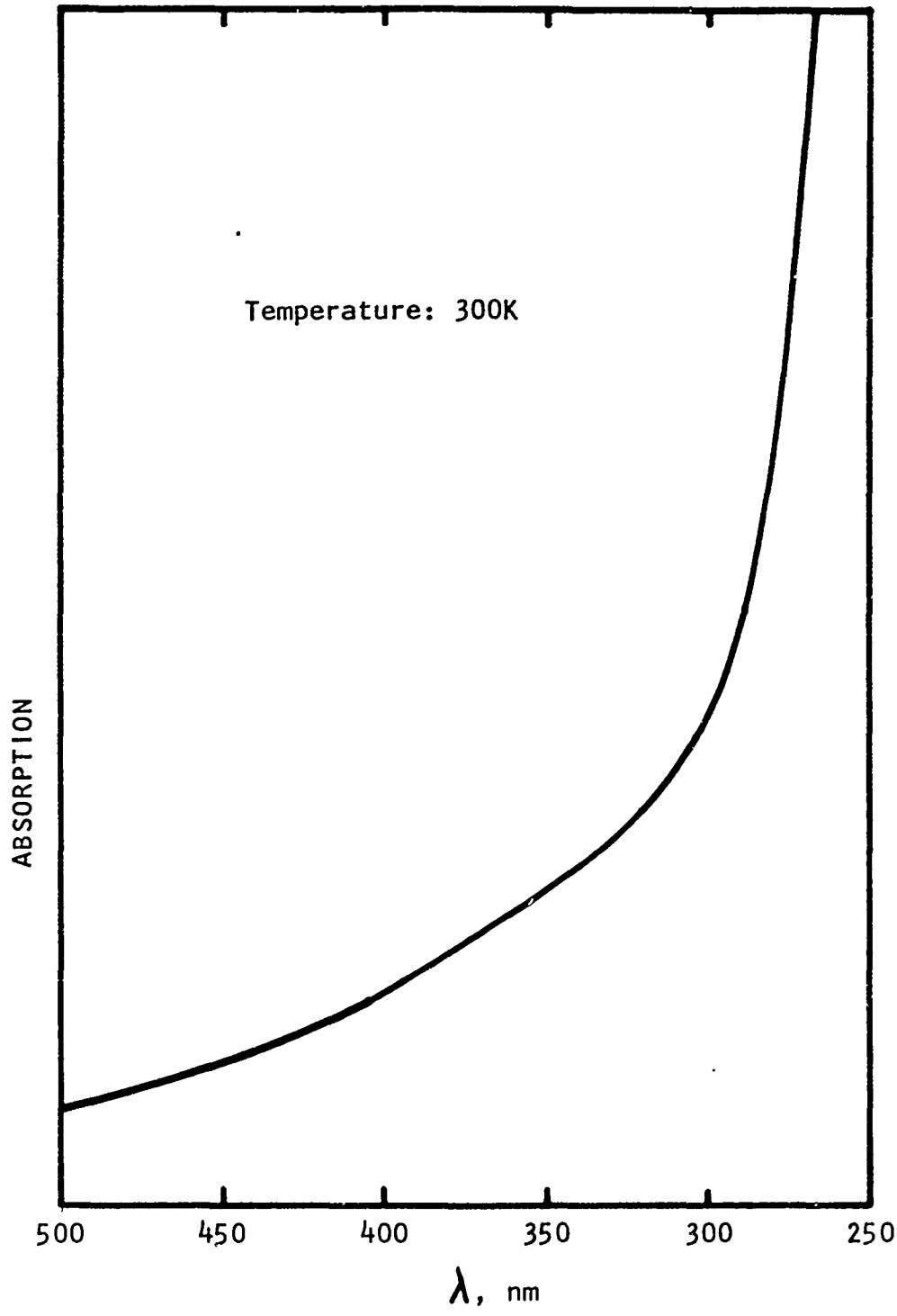

Fig 6 Absorption of RDX single crystal, derived from specular reflectance data

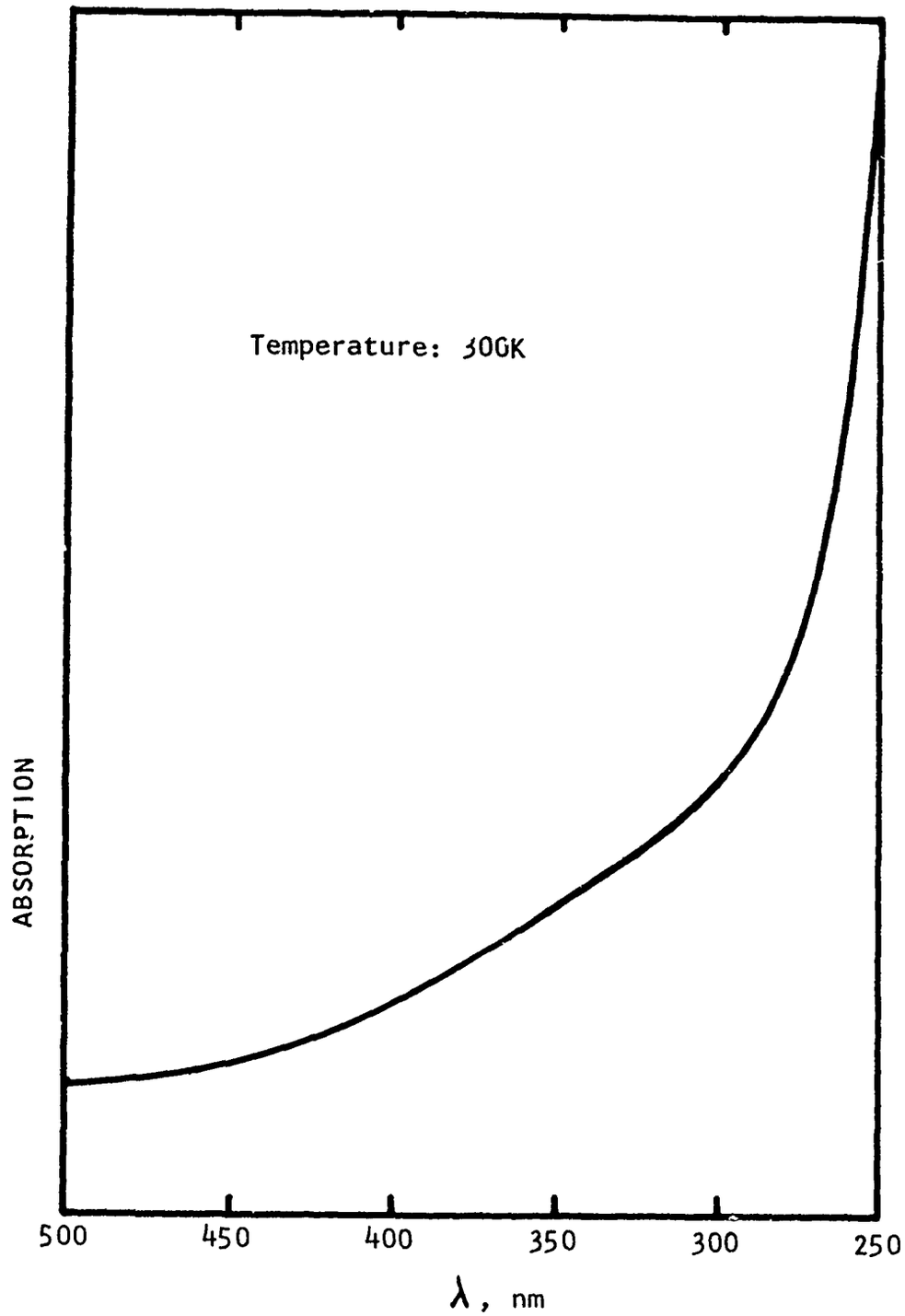

Fig 7 Absorption of HMX single crystal, derived from specular reflectance data

The tabulated data from which Figures 6 and 7 were plotted were graphed as a function of $\Delta\lambda$ on a semilogarithmic plot, as shown in Figure 8 for the case of RDX. The origin is taken at the peak of the strong nitramine band, which from the reflectance data is 255 nm in the solid. It is seen that in the region 325-425 nm, corresponding to $\Delta\lambda$ = 70-170 nm, the tail is to a good approximation exponential. The value of A was then evaluated from the intercept at $\Delta\lambda = 0$, and B was obtained from the slope. With these constants, Equation (8) is the theoretical expression for the Urbach tail of the nitramine band.

The values of ε calculated from Equation (8) were then subtracted from the experimental values. This difference is shown in Figures 9 and 10 for RDX and HMX, respectively (the vertical scale has been exaggerated for clarity). It is seen that after subtraction of the Urbach tail, there remains in each case a skewed absorption band peaking at about 350 nm for HMX, and 365 nm in RDX. There is also a slight suggestion of some structure near 380 nm. These characteristics will subsequently be shown to be repeated in the excitation spectra for fluorescence and phosphorescence.

Although our interest lies with the weak 340 nm band, it is found from the reflectance data that the nitramine band peaks at 255 nm in RDX and 245 nm in HMX crystals. When compared with the corresponding values of 236 nm (Ref 5) and 226 nm (Ref 25) in acetonitrile solution, it is seen that this band exhibits a substantial blue shift upon solvation. We will return to this point below.

Transmission Spectra of Thin Single Crystals

Transmission spectra of both RDX and HMX thin single crystals (Ref 28) are shown in Figures 11 and 12. Absorption is seen to continue out to 400 nm, but no band can be definitely identified near 340 nm. The absorption tailing out to 400 nm may be due to scattering by the crystal surface imperfections. However, these spectra are useful for establishing the maximum molar extinction coefficient, ε, to be expected for a band near 340 nm. One can use the definitions of absorption coefficient, α, and molar absorptivity to show that

$$\varepsilon = \alpha/2.303\ C \qquad (9)$$

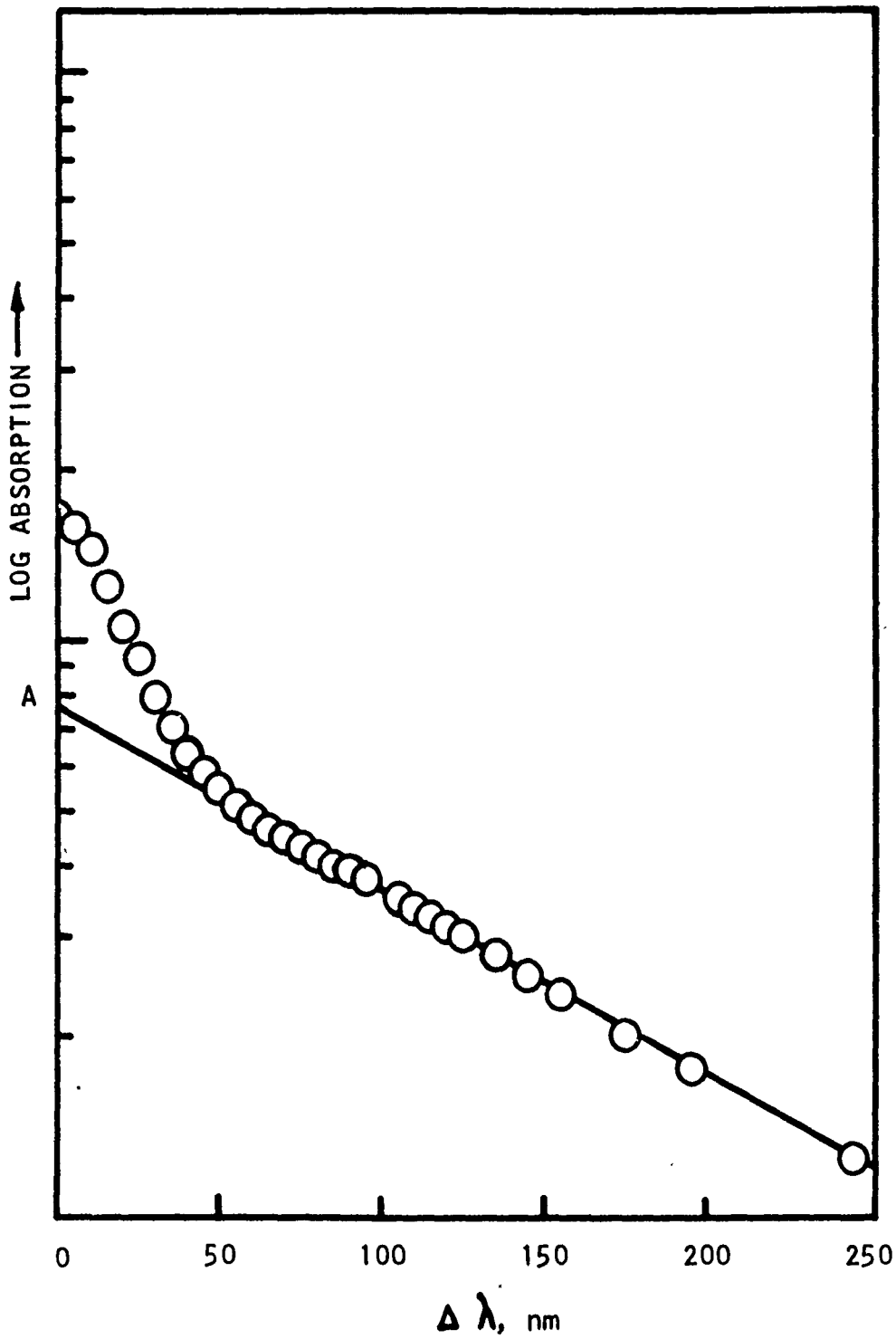

Fig 8 Urbach Tail of nitramine band in RDX, derived from specular reflectance data

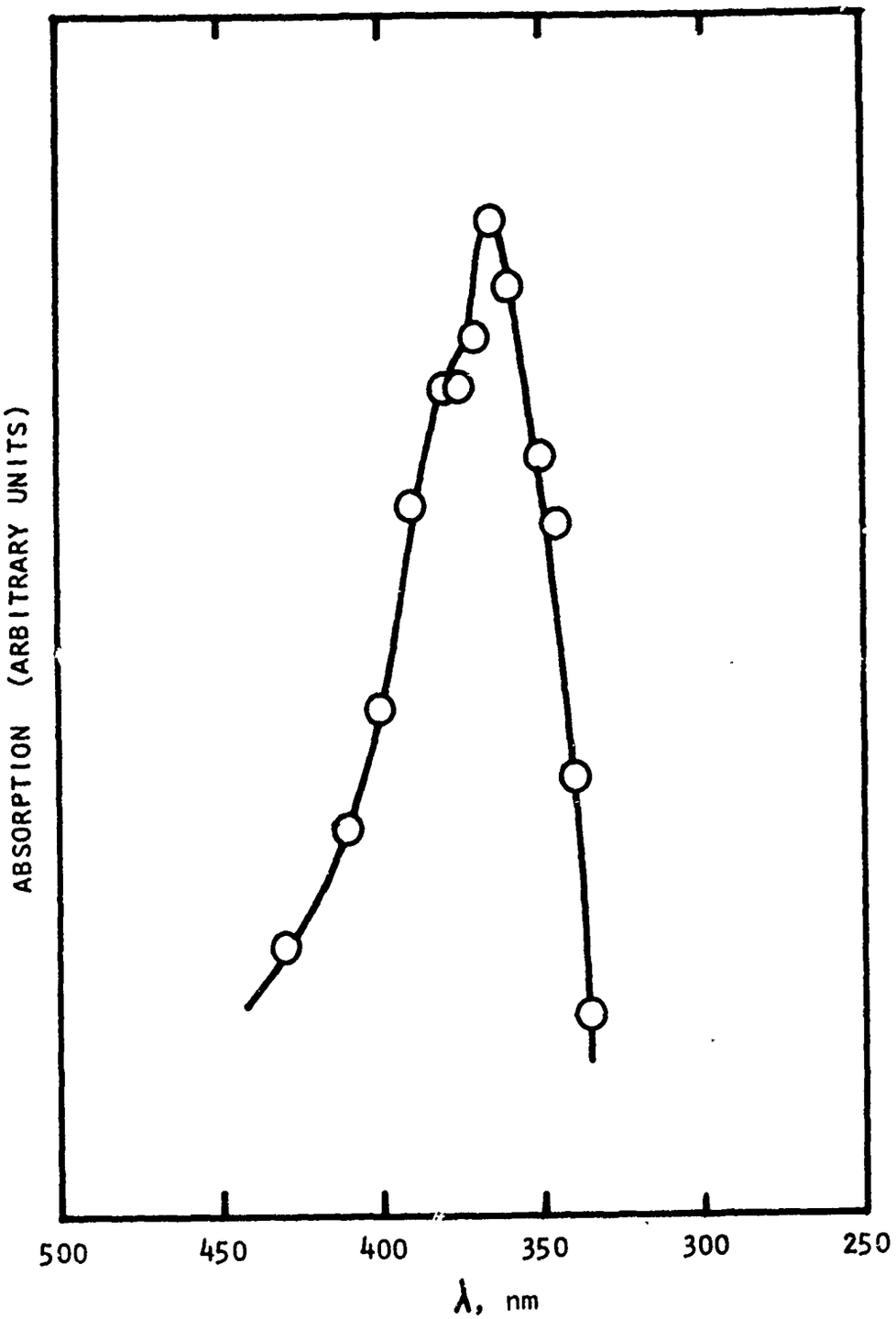

Fig 9 Absorption of RDX single crystal, after subtraction of Urbach Tail

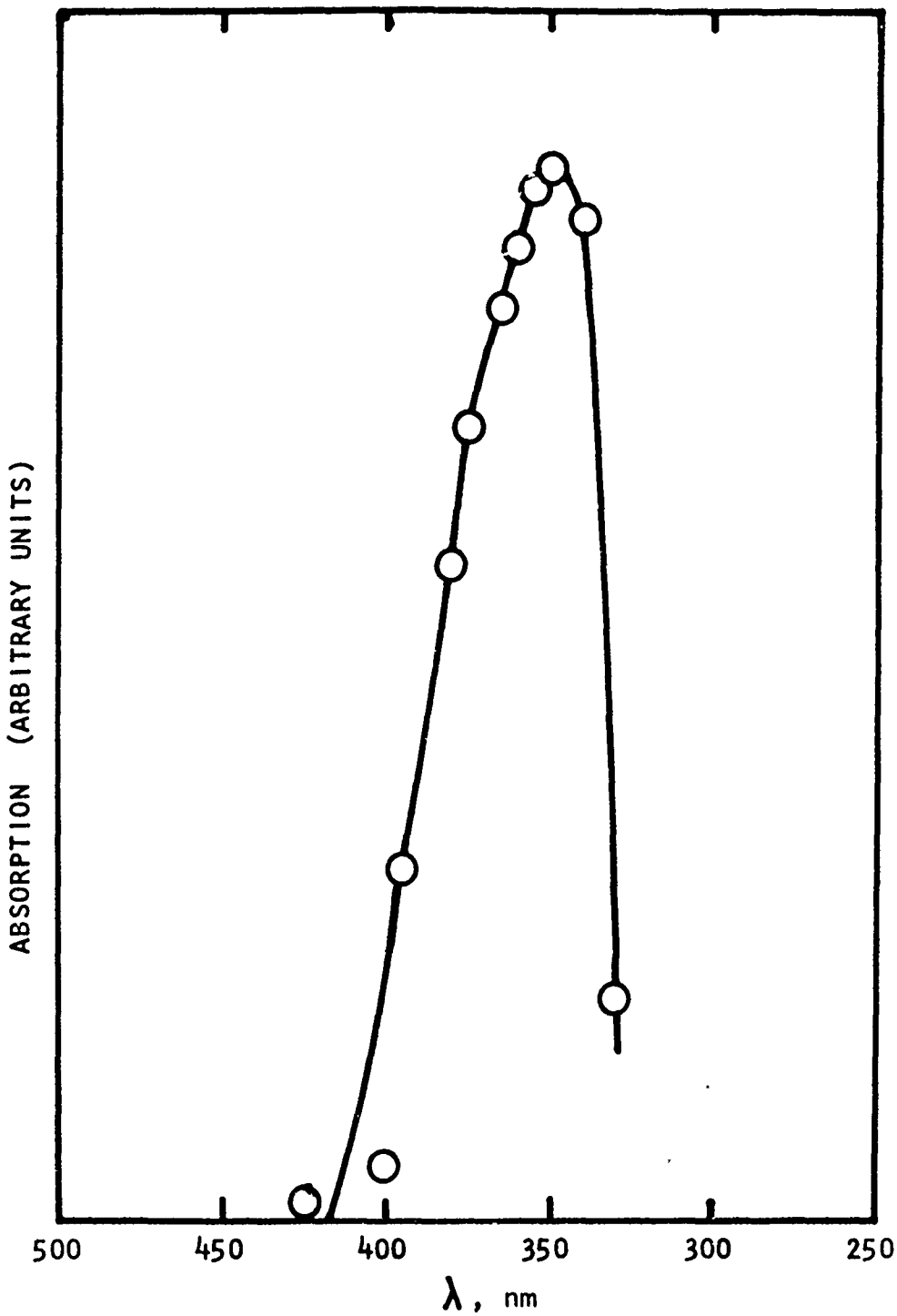

Fig 10 Absorption of HMX single crystal, after subtraction of Urbach Tail

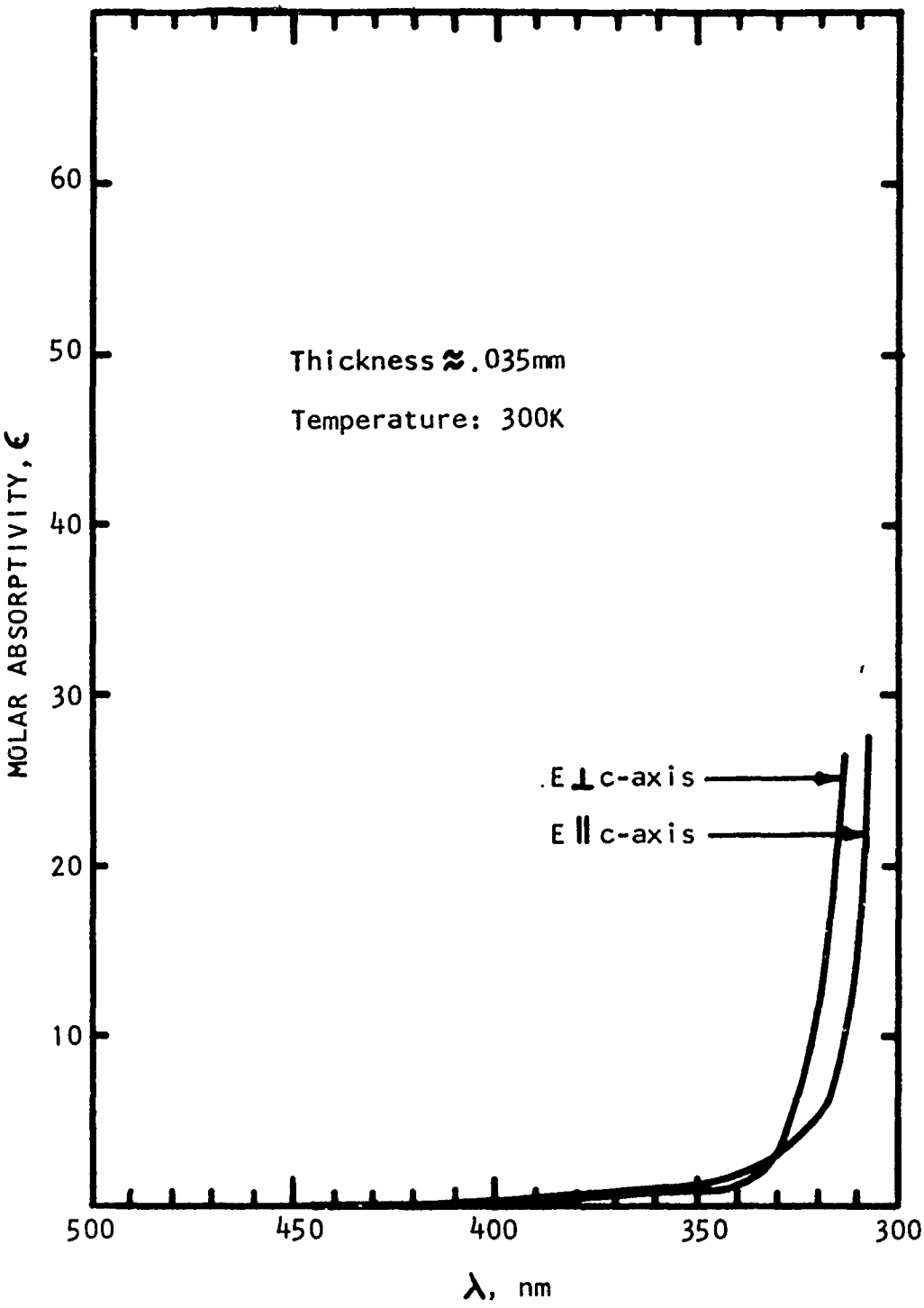

Fig 11 Absorption spectrum of thin RDX crystal

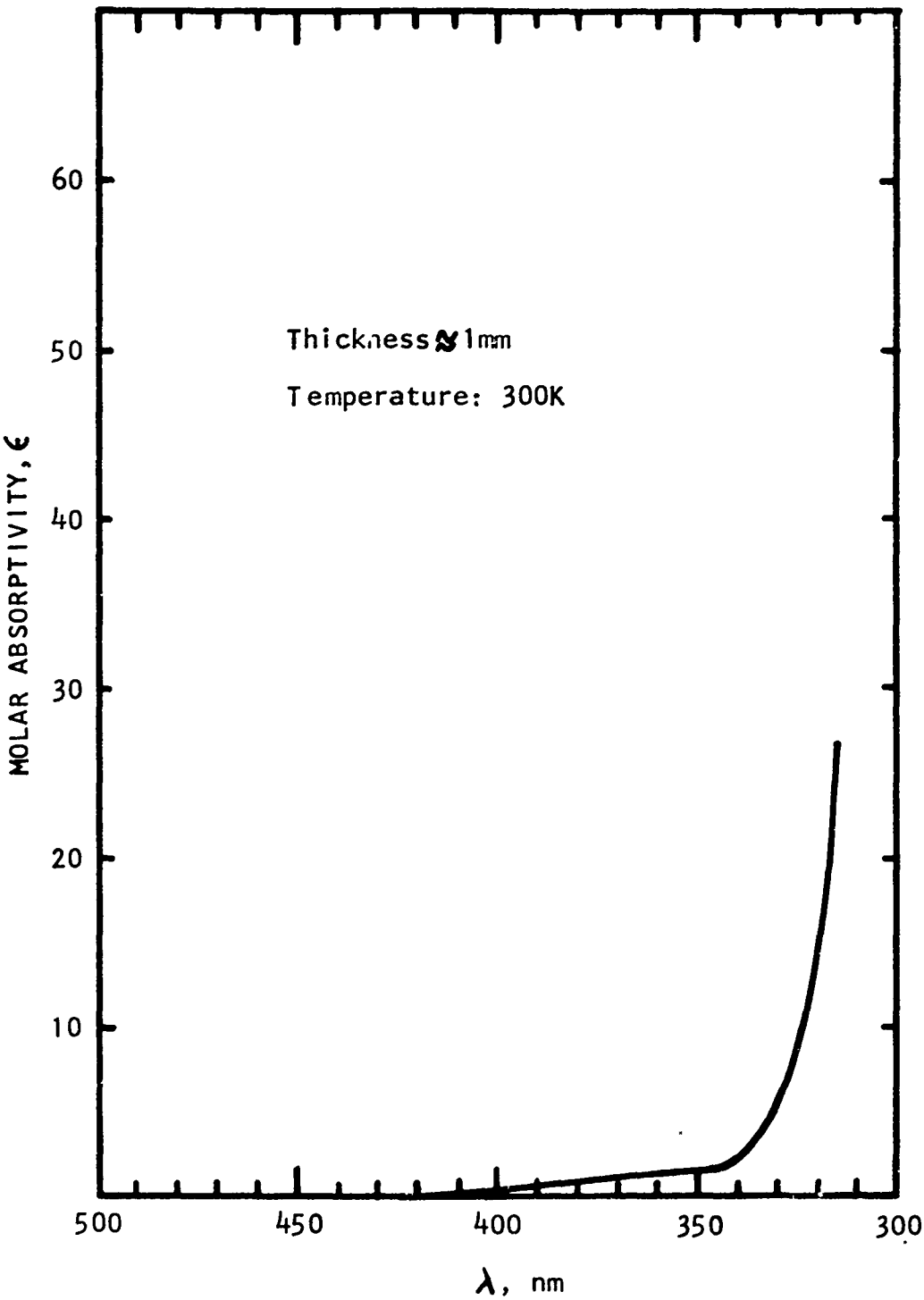

Fig 12 Absorption spectrum of thin HMX crystal

Where C is the concentration in moles/liter. Converting from concentration to the density, d, of the solid using the molecular weight, W, one has

$$\varepsilon = \alpha W \times 10^{-3}/2.303\ d. \qquad (10)$$

Using the values W = 222 and d = 1.8 g/cc, the equivalent molar absorptivity at 340 nm is approximately 1, or about .006% as great as at 195.5 nm, where $\varepsilon = 16{,}400\ M^{-1}cm^{-1}$. Thus, any measurement on a solution dilute enough to display the 195.5 nm band is certainly too dilute to show the band at 340 nm. Similar results are obtained for HMX using W = 296 and d = 1.9 g/cc. These upper limits are of importance because Stals has used the absence of a 340 nm band in his solution spectra to argue that this absorption is peculiar to the solid state of RDX. It is apparent that more concentrated solutions are necessary in the search for this band.

Maycock, et al, have obtained transmission spectra for an HMX single crystal at 77K which show structure on the absorption tail between 320 and 420 nm (Ref 29). Their data are reproduced in Figure 13. The thickness of the crystal was not noted, so that the absorptivity at 340 nm could not be determined. Since these authors found no evidence of this structure in the transmission spectrum of a .034 M solution of HMX in acetone, they attributed it to a solid state effect. Again, however, such a solution would be too dilute to allow detection of a band for which we now expect $\varepsilon \approx 1$. The low solubility of HMX limits the maximum achievable concentration, and from these results alone it is unclear whether the 340 nm band has a solid state origin.

Absorption Spectra of Concentrated Solutions

In an effort to resolve this question, we have repeated these measurements using saturated solutions of RDX and HMX in acetonitrile. Special sample cells were used to obtain a path length of 10 cm. The results are shown in Figures 14 and 15, where it can be clearly seen that at 340 nm the molar absorptivity is of the order of .05, some 20-30 times smaller than at the same wavelength in the single crystal spectra. There is no discernible band in this region for solvated RDX or HMX.

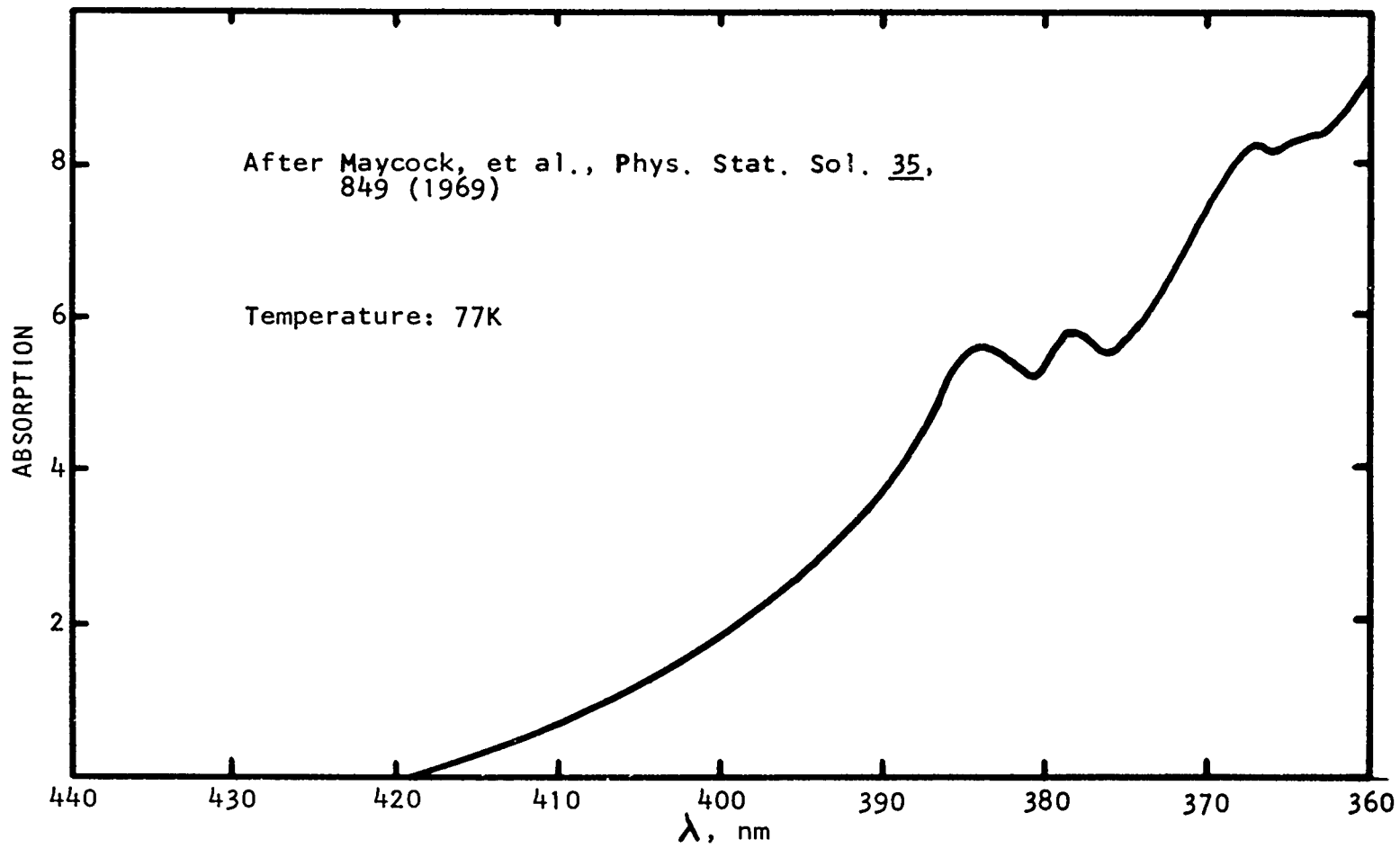

Fig 13 Absorption spectrum of HMX thick single crystal

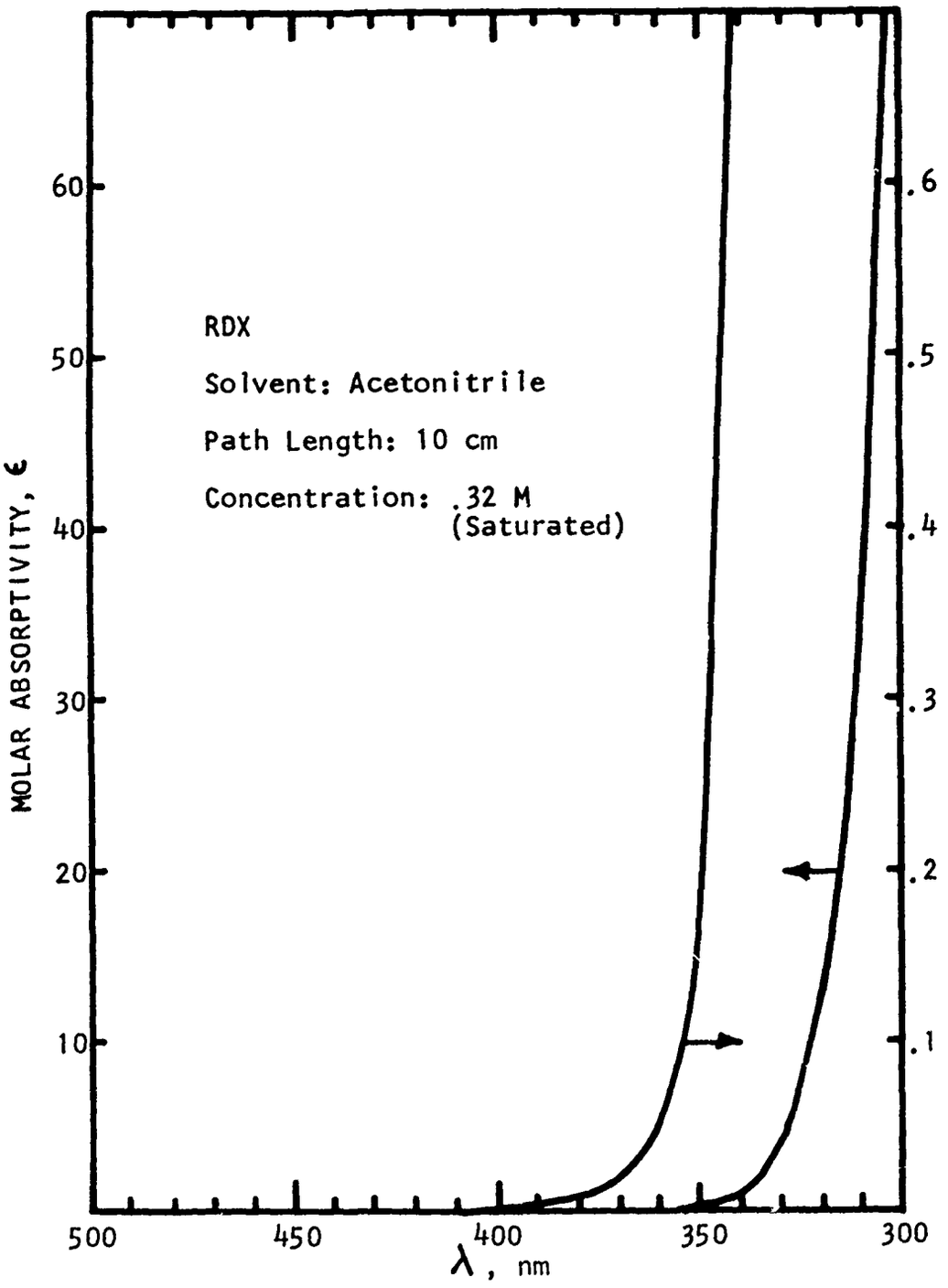

Fig 14 Absorption of RDX in solution

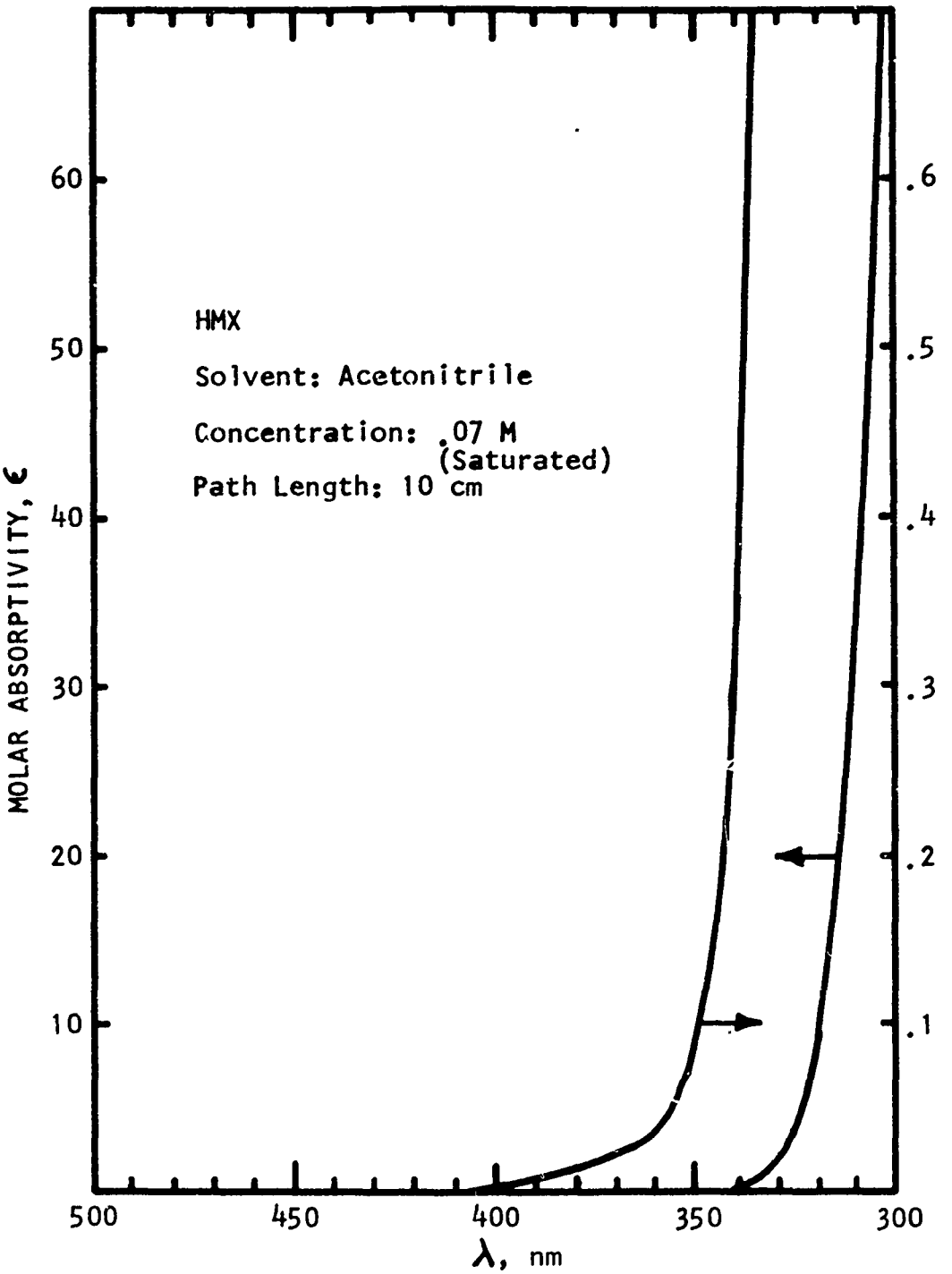

Fig 15 Absorption of HMX in solution

One can imagine three possible explanations for this negative result:

1. If the nitramine band were red shifted in going from the solid to the solvated state, it could obscure the weaker 340 nm band,

2. In solution the 340 nm band might shift to shorter wavelengths, and be hidden under the nitramine band, or,

3. The 340 nm band observed in crystalline samples could be a true solid-state effect.

The first possibility can be eliminated by noting that as seen above, the nitramine band is blue shifted in going from the solid to the solvated state, by about 20 nm for both RDX and HMX.

Circular Dichroism Spectra

With regard to the second possibility, if the 340 nm band had shifted to shorter wavelengths, it might possibly be uncovered by the use of circular dichroism spectroscopy. This technique measures the difference in absorption of right- and left-circularly polarized light and is sometimes useful in discerning weak bands hidden under strong ones. An example of the power of this technique is found in the work of Djerassi, et al, (Ref 30) who used it to reveal the presence of a weak band near 340 nm in certain nitro-steroids. No satisfactory explanation for this anomalous band has yet been advanced.

Circular dichroism spectra of both RDX and HMX in acetonitrile solution were recorded on a Carey Model 60 CD spectrometer at the Department of Chemistry at New York University. For different wavelength intervals, different concentrations were used to keep the molar absorptivity within the limits for optimum sensitivity of the technique.

No Cotton effect was found in the CD spectra in the wavelength interval 200-450 nm. Not only does this result not indicate the presence of a 340 nm band in solution, but that the nitramine band in both RDX and HMX does not display a Cotton effect.

We must therefore conclude that the weak band observed in the absorption spectra derived from the specular reflectance measurements on RDX and HMX single crystals is indeed due to some solid-state effect. Stals (Ref 27) has discussed the possibility that this band is either the nitramine band, red shifted by crystallization, or a Davydov component of the nitramine band, red shifted by resonance interaction. As for the first possibility, we have already seen above that the red shift of the nitramine band upon crystallization amounts to 20 nm, which, although substantial, is far too small to shift it to 340 nm. The second hypothesis requires a Davydov splitting of at least 12000 cm^{-1} toward the red from the position of the nitramine band in the solid (Stals obtained a value of 12,000 cm^{-1} based on the position of the weak band at 330 nm). This value seems unreasonably large, as will be discussed further in the section entitled Discussion.

Since the transmission spectra of thin single crystals do not seem to show the 340 nm band clearly, it seems possible that it is a property of the crystal surface which is sampled in the reflectance measurement. In this connection it is interesting to examine the transmission spectra of evaporated films of RDX and HMX published by Maycock, etal, (Ref 29) which are reproduced in Figure 16. Such films are expected to have a high density of defects, such as would be present at the surface of a single crystal. The spectra show absorption in the region 320-400 nm which is much more prominent with respect to the nitramine band than it is in the thin single crystal spectra of Figures 11 and 12. It therefore seems possible that the 340 nm band is associated with the formation of defects at the surface of the crystal, and would therefore figure prominently in the luminescence properties of powdered samples in which the surface-to-volume ratio is very large.

Fluorescence and Fluorescence Excitation

The fluorescence and fluorescence excitation spectra of RDX_{p-6} and HMX_{p-8} are shown in Figures 17 and 19, respectively. The excitation spectra of these protonated samples are in excellent agreement with the absorption spectra of Figures 9 and 10. The corresponding spectra for deuterated samples are shown in Figures 18 and 20. These samples could not be recrystallized due to the small quantities available, and may not be as pure as the protonated materials. The excitation efficiency drops to near zero at wavelengths where the isolated molecule absorbs appreciably (see Fig 14 and 15).

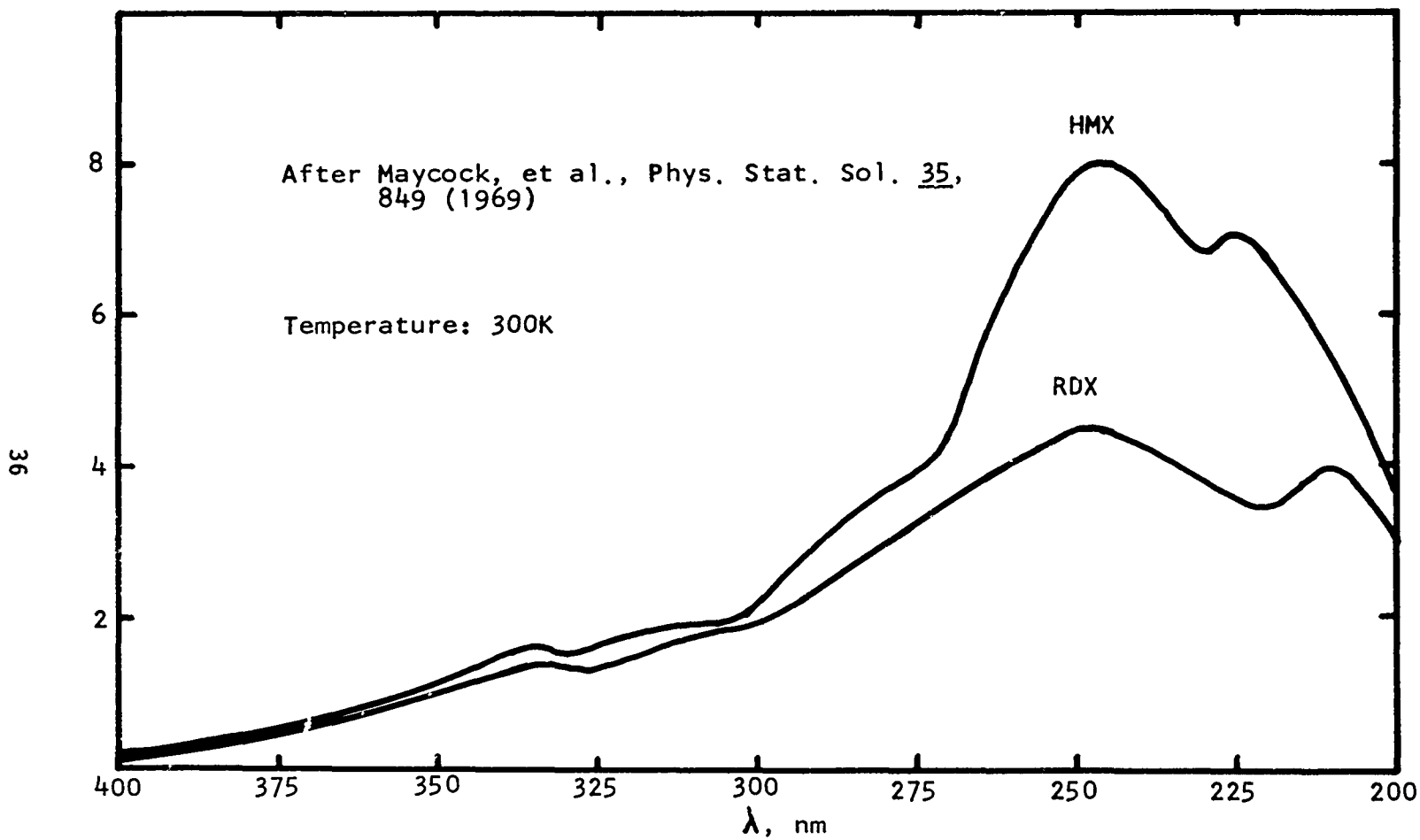

Fig 16 Absorption of thin films of RDX and HMX

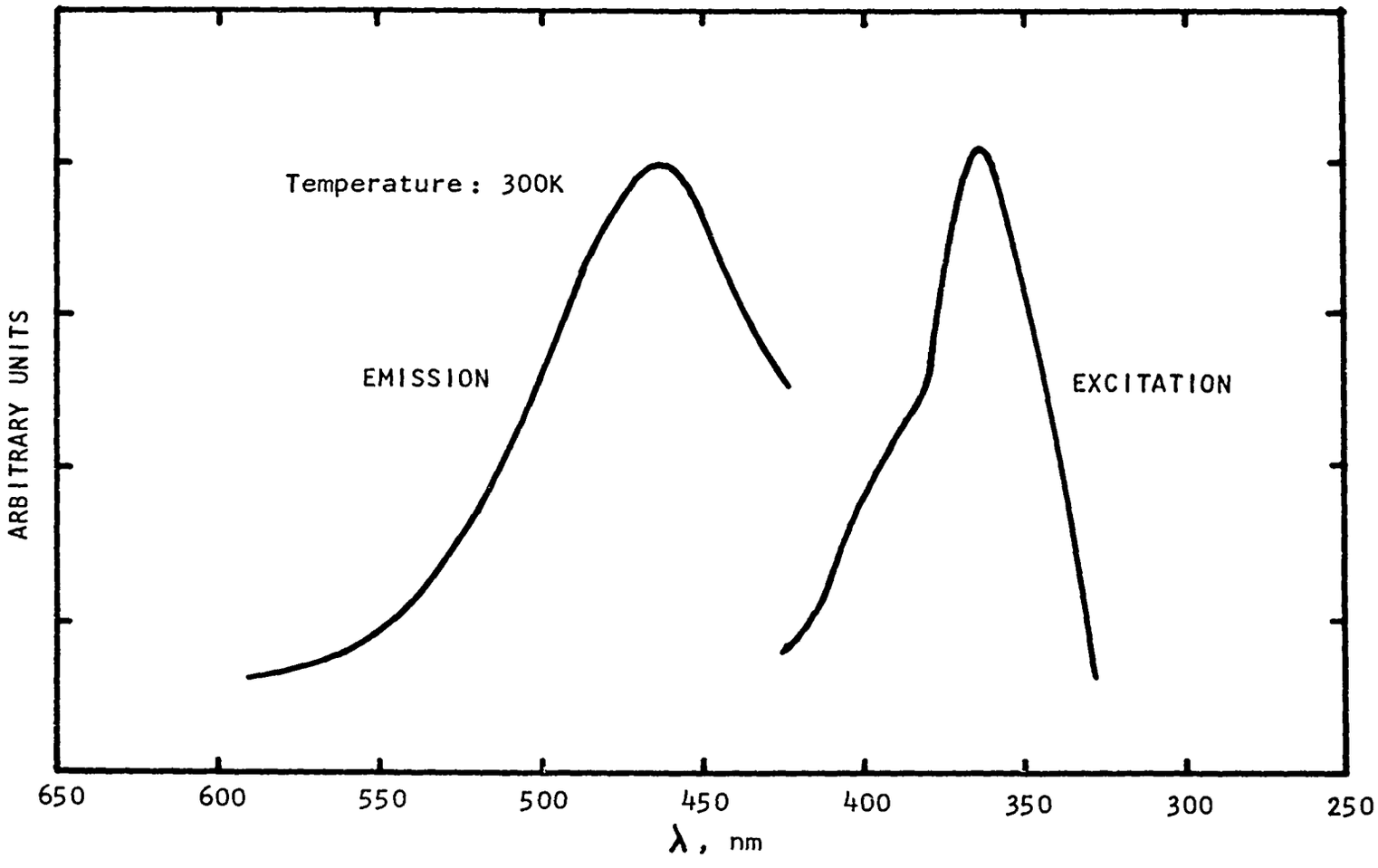

Fig 17 Fluorescence and fluorescence excitation of RDX_{p-6}

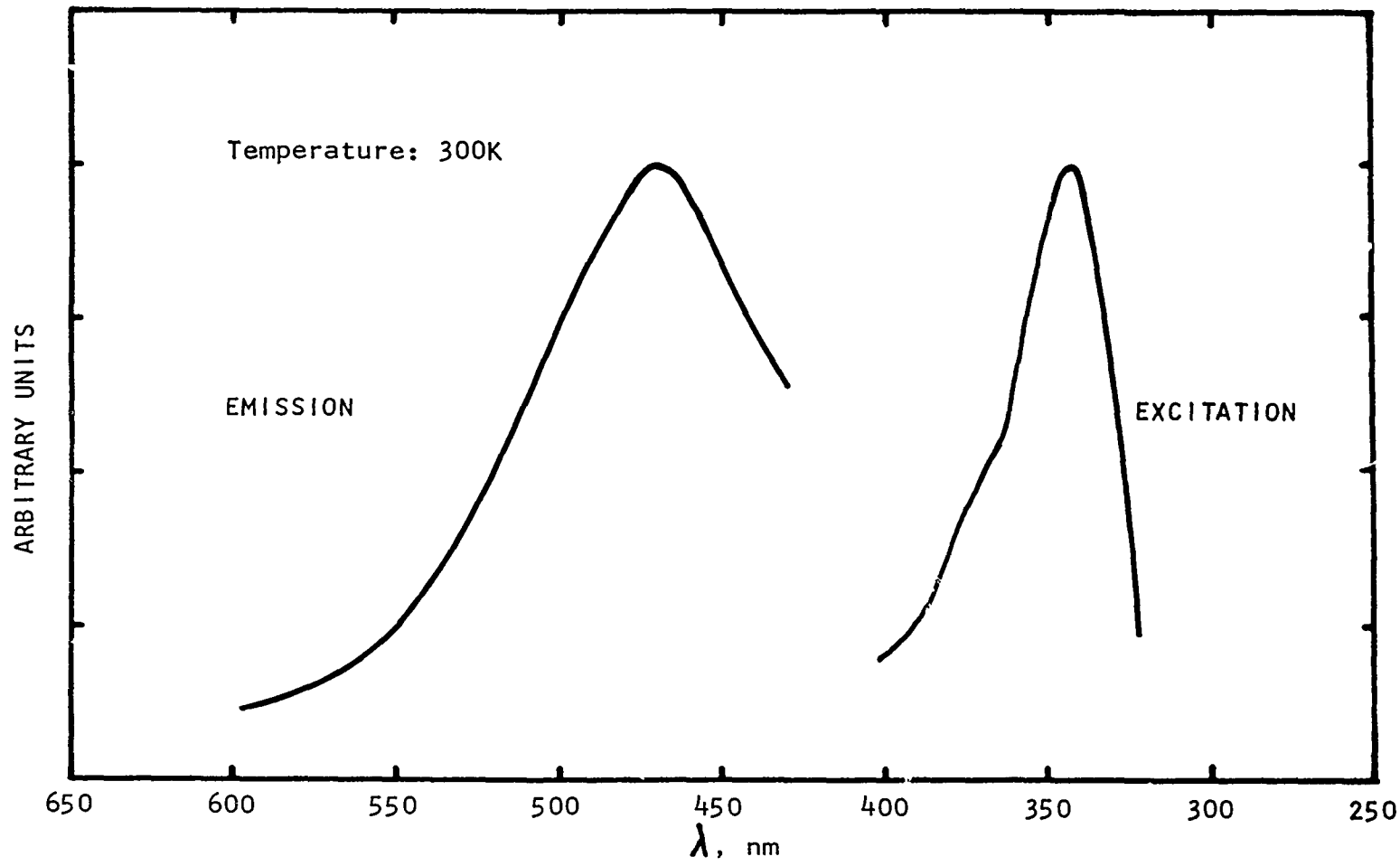

Fig 18 Fluorescence and fluorescence excitation of RDX_{d-6}

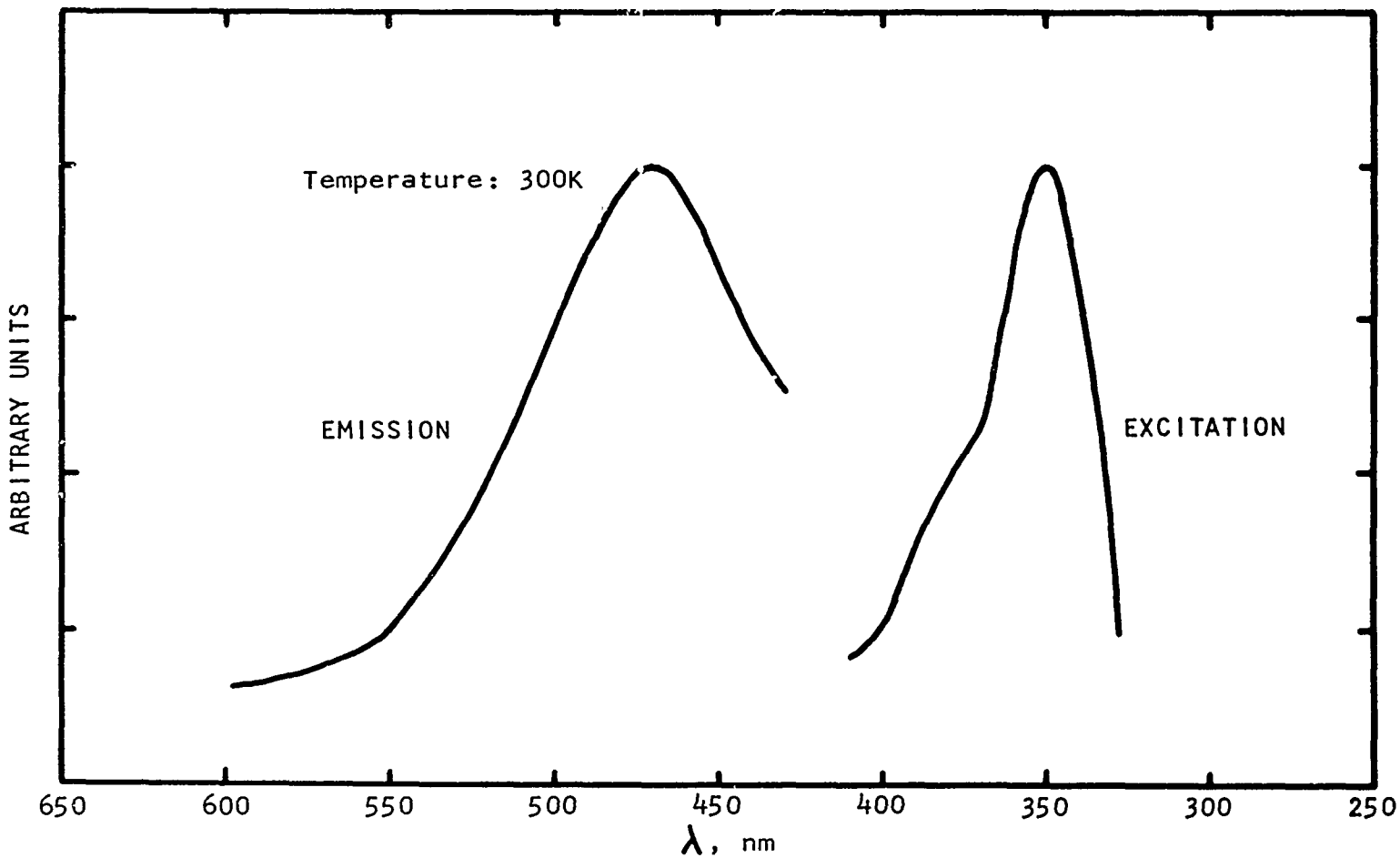

Fig 19 Fluorescence and flouorescence excitation of HMX_{p-8}

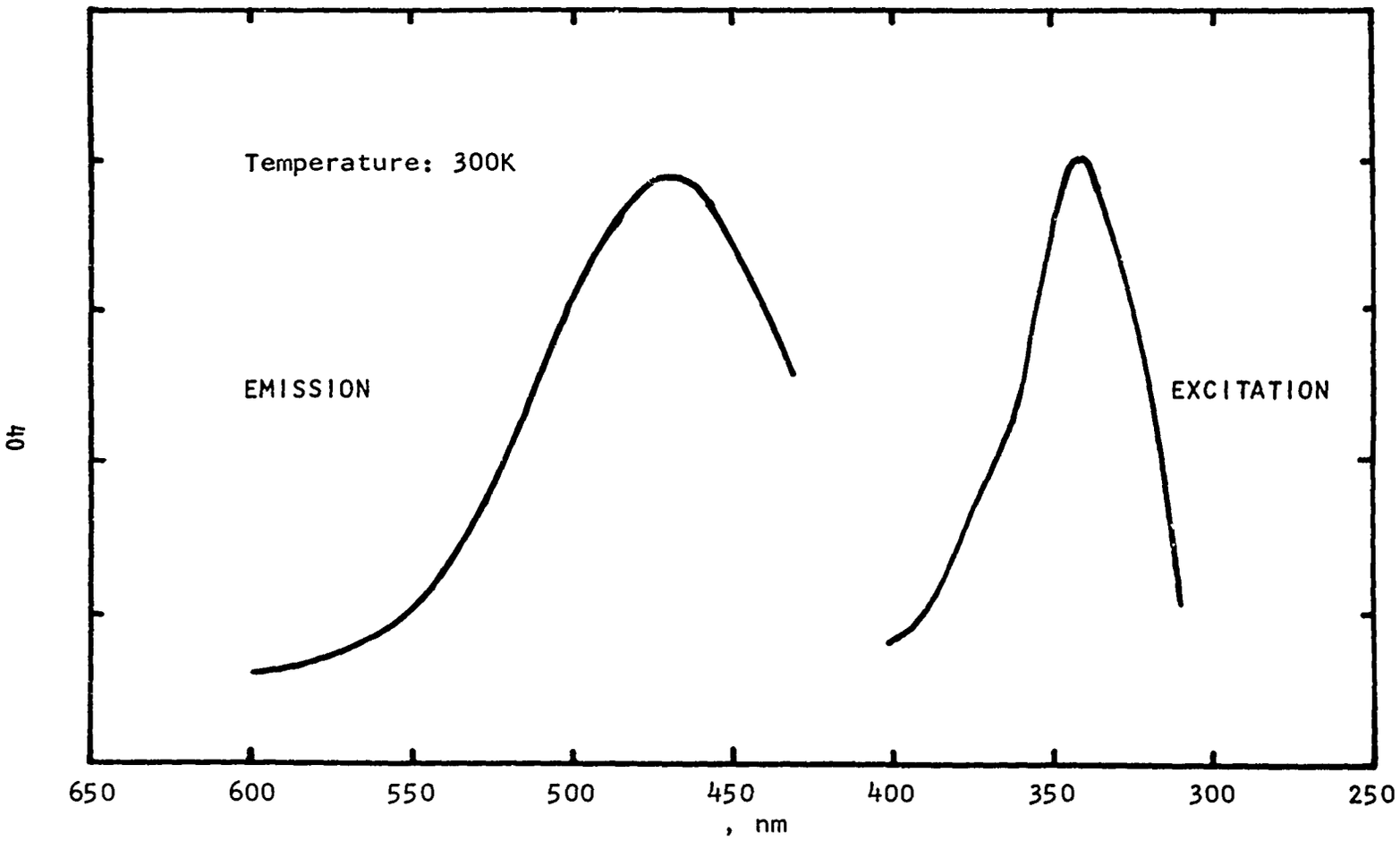

Fig 20 Fluorescence and fluorescence excitation of HMX_{d-8}

The emission spectra peak near 465 nm, and continue out to about 600 nm. Since the samples were in solid form, the amount of excitation light which was scattered into the analyzing monochromator was more intense than it would have been with a sample in the form of a solution. For this reason, emission spectra could not be measured below about 425 nm, and excitation spectra above about 410 nm.

Fluorescence and fluorescence excitation spectra normally are in a mirror-image relationship to one another, i.e., there is a wavelength about which one is symmetrically disposed with respect to the other (Ref 1). In the present case, this relationship is not obvious, due to the abrupt short-wavelength cutoff of the excitation spectra at 320 nm. This cutoff is believed to be due to strong absorption by the nitramine band, and is discussed further in section entitled Discussion. Estimation of the mirror-image wavelength is further hampered by the limits placed on the ranges over which the spectra could be measured. However, a rough estimate places it near 400 nm, corresponding to an energy of 3.1 eV.

The fluorescence decay was measured at room temperature using the photon counting apparatus described in section entitled Experimental. Excitation was at 340 nm and the viewing filter was a Corning No. 3-73 glass filter which passes wavelengths longer than about 420 nm. The fluorescence of this filter determined the shape of the "lamp profile" shown as a solid line in Figure 21, which was measured using a non-fluorescent sample of MgO. The early portion of this profile has a decay time of about 3.5 ns, which may be considered the response time of the system.

Figure 21 shows a slight deviation of the RDX and HMX fluorescence decay from the "lamp profile" for times greater than about 20 ns. It is difficult to tell whether this represents a real effect, since it occurs where the fluorescence intensity has decreased to a value comparable to the system noise. In any case, it is probably safe to say that most of the sample fluorescence is emitted with a characteristic lifetime of less than 3.5 ns, since there is no deviation of the experimental curves from the early part of the "lamp profile".

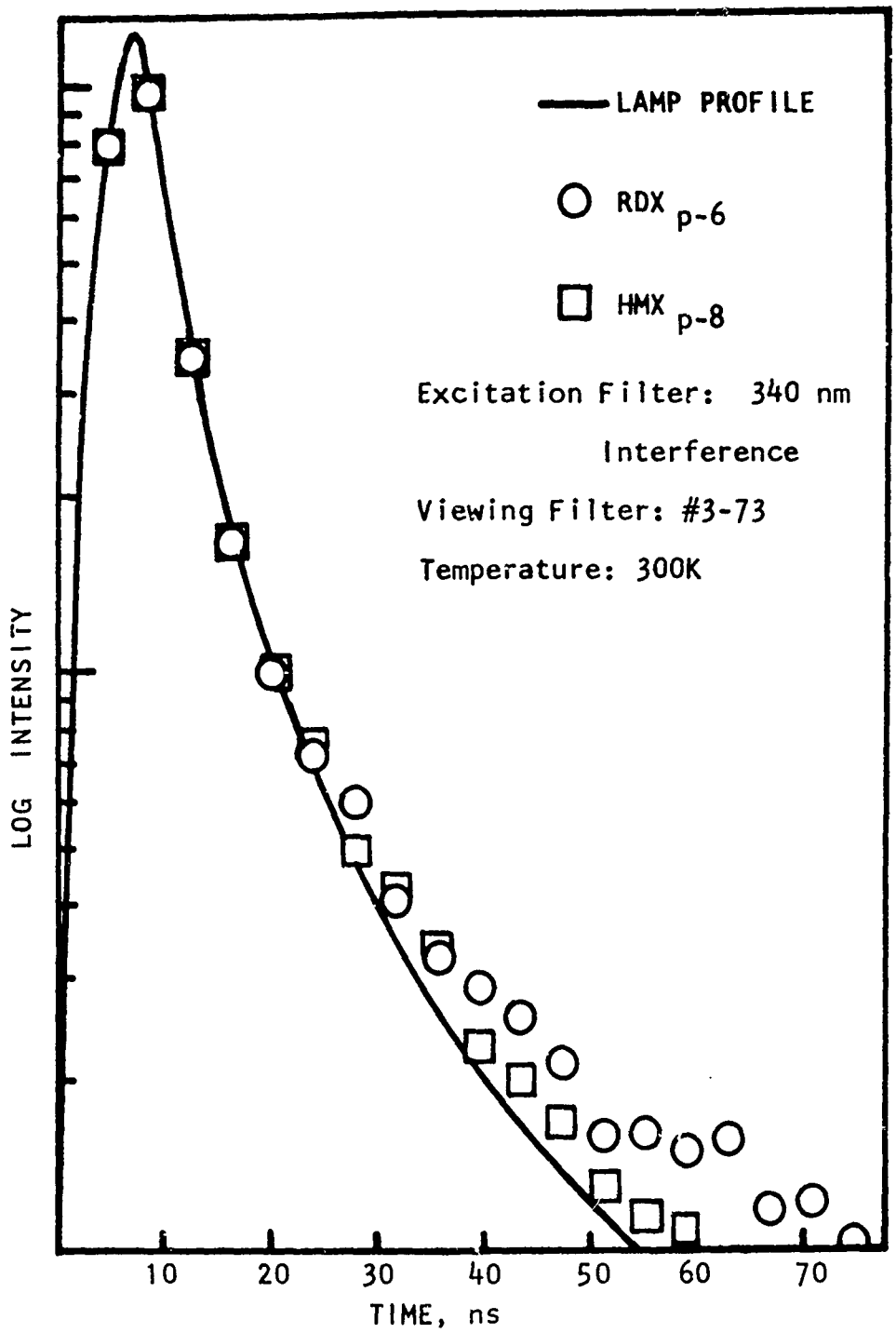

Fig 21 Fluorescence decay of RDX and HMX

Phosphorescence and Phosphorescence Excitation

The phosphorescence and phosphorescence excitation of RDX_{p-6} and HMX_{p-8} are shown in Figures 22 and 23, respectively. The excitation spectrum in both cases is a skewed curve beginning near 400 nm, peaking at 340 nm, and dropping sharply to zero at 320 nm. A similar drop in fluorescence excitation efficiency at this wavelength was noted earlier. The phosphorescence excitation peak wavelength is close to that of the fluorescence excitation peak, and to the absorption maximum observed in the data derived from the reflectance spectra of single crystals as shown in Figures 9 and 10. The slight bump in the excitation spectra of both RDX and HMX at 375 nm is reproducible and appears to correspond to a similar feature in the fluroescence excitation spectra of Figures 17 and 20, and also appears to have a counterpart in the absorption spectra of Figures 9, 10, and 13.

Similar results were found for deuterated RDX and HMX and are shown in Figures 24 and 25. The temperature of measurement for all samples was 77K.

The emission spectrum is in each case a broad structureless Gaussian-like curve peaking at 520 nm. By comparison with the fluorescence emission spectra of Figures 17-20 it is evident that there is a good deal of overlap between the fluorescence and phosphorescence emission spectra.

Phosphorescence decay curves were measured with the apparatus described in section entitled Experimental at 77K. A Corning No. 3-68 glass color filter was used as the viewing filter and passes wavelengths longer than about 530 nm. This cutoff wavelength was chosen to limit as much as possible the response of the photomultiplier to wavelengths due to phosphorescence and to reject wavelengths which could conceivably be due to thermally stimulated fluorescence. The measurements were repeated using a No. 3-70 filter which passes wavelengths longer than about 490 nm. No difference in the results was noted and therefore it is concluded that no contribution to the measured decay curves was due to delayed thermal fluorescence.

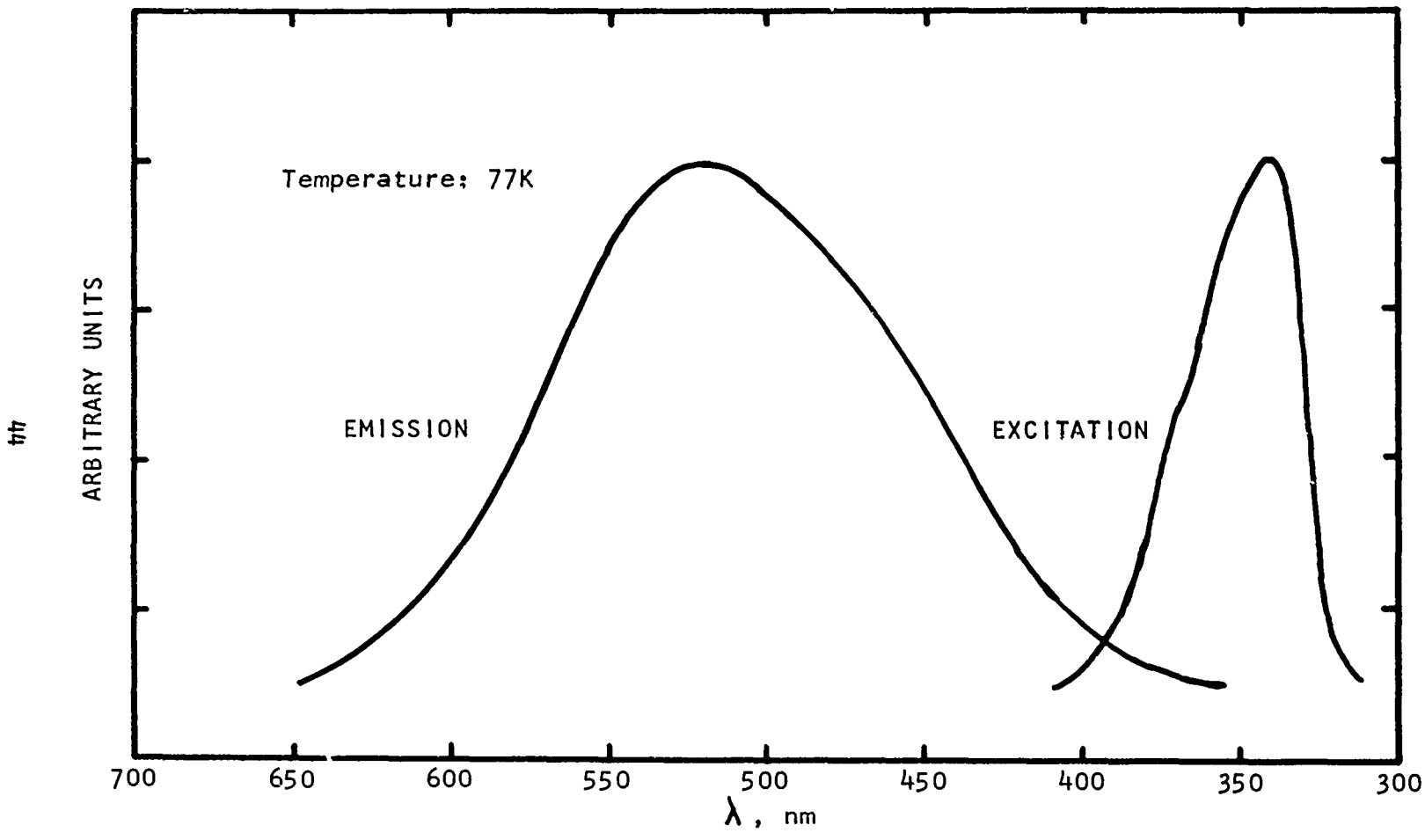

Fig 22 Phosphorescence and phosphorescence excitation of RDX_{p-6}

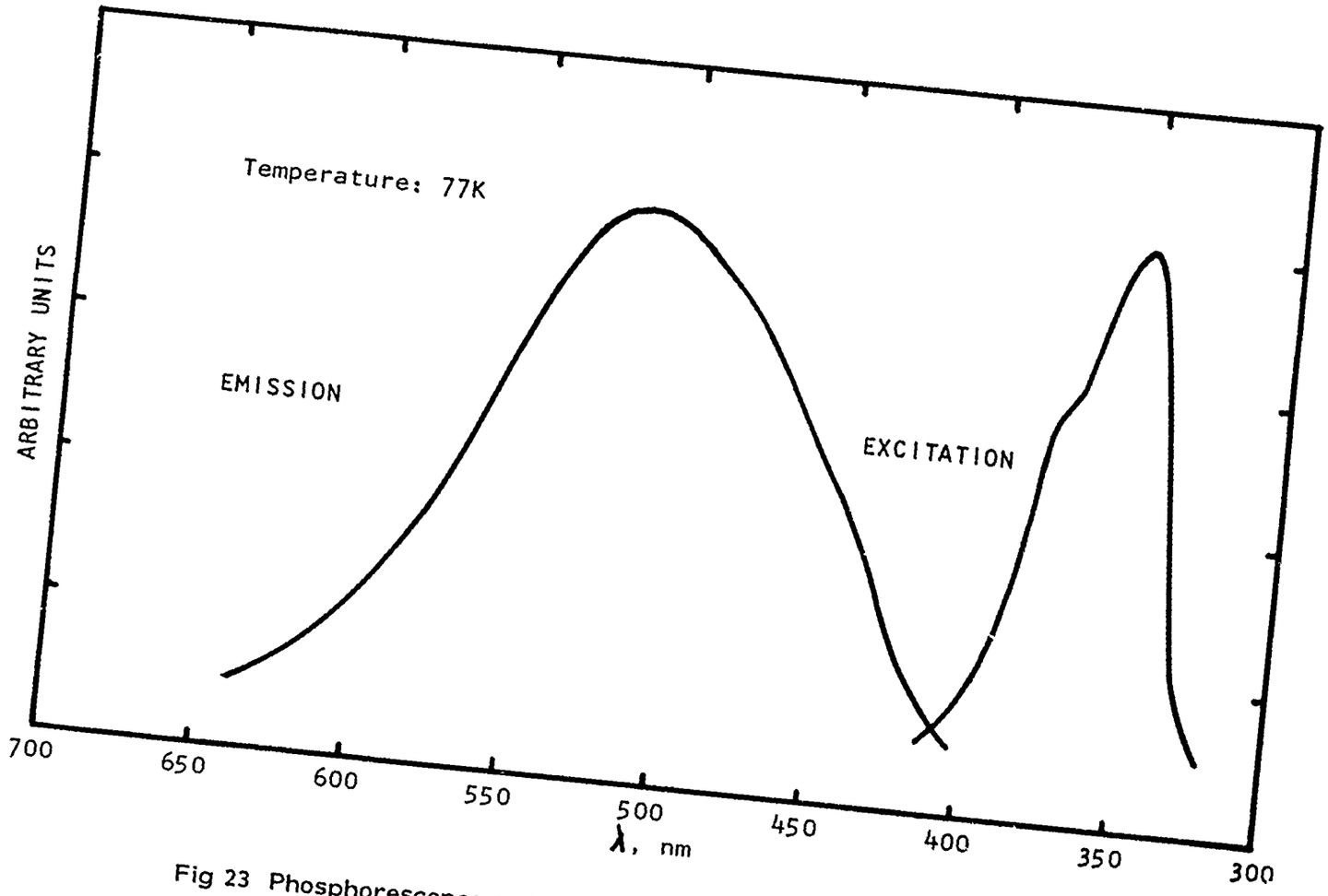

Fig 23 Phosphorescence and phosphorescence excitation of HMX_{d-6}

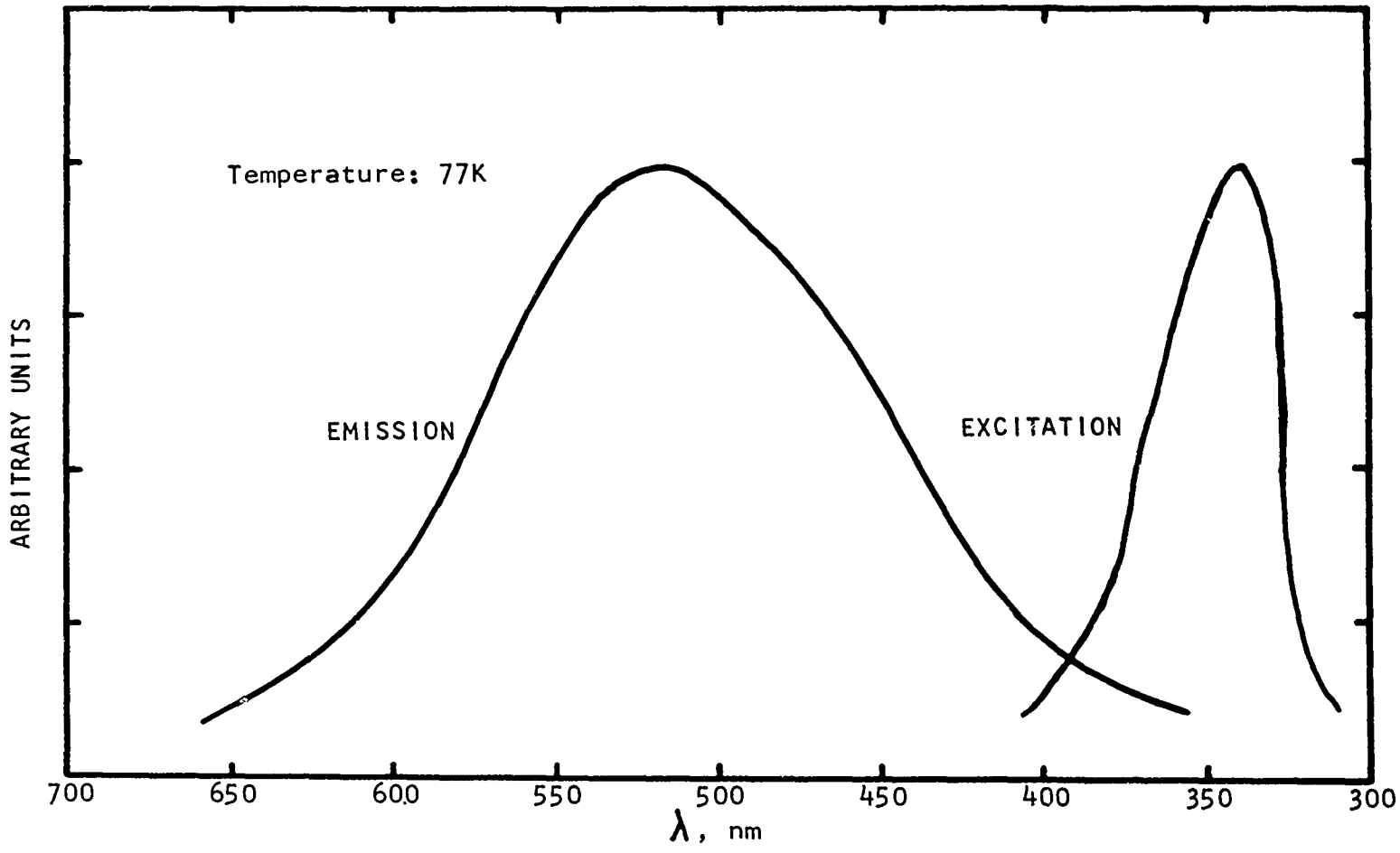

Fig 24 Phosphorescence and phosphorescence excitation of RDX_{p-8}

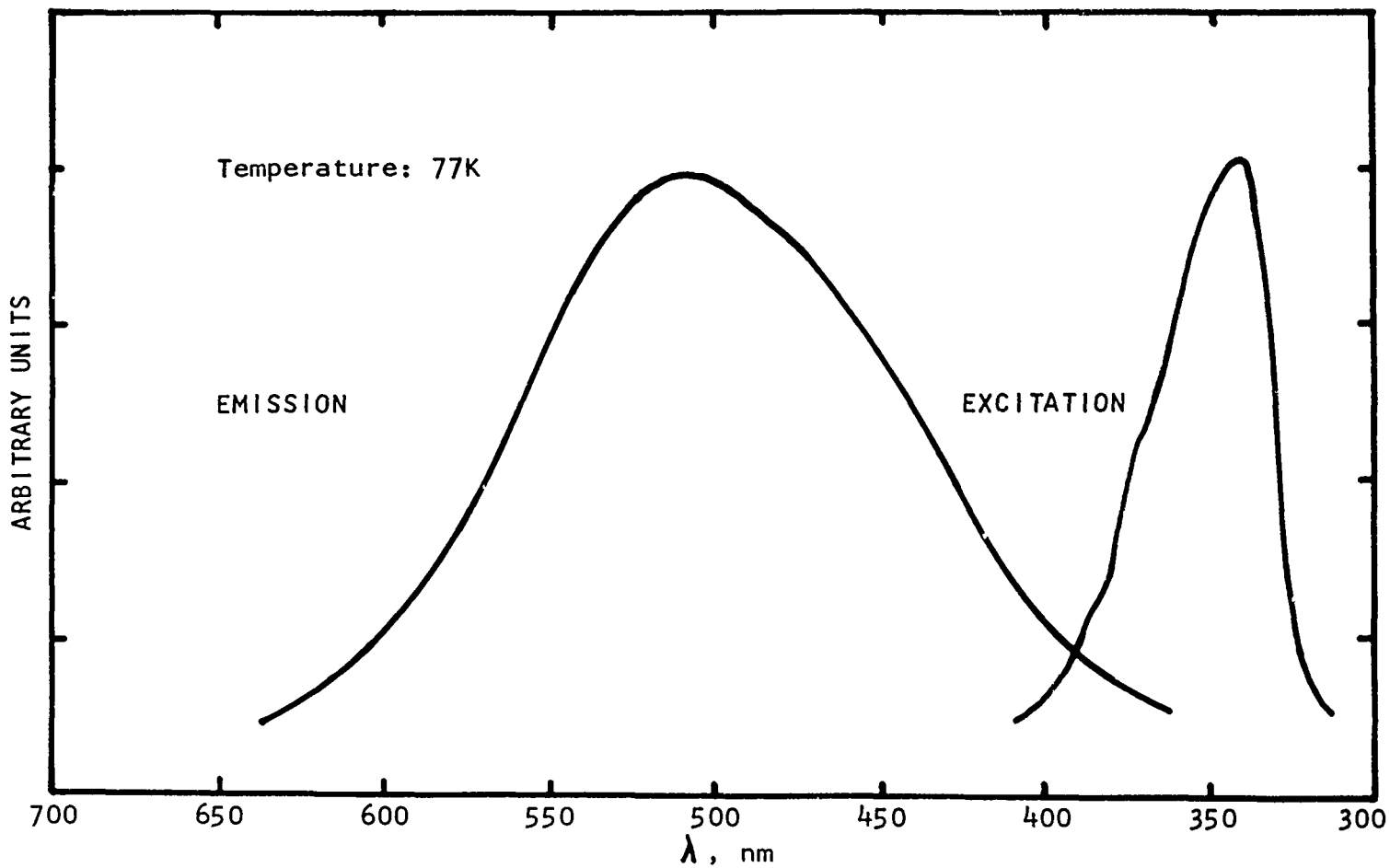

Fig 25 Phosphorescence and phosphorescence excitation of HMX_{d-8}

The phosphorescence decay was found to be nonexponential. This occurs when the total decay curve is a superposition of more than one exponential decay, each decay having its own characteristic intensity and each with its own characteristic lifetime. If the number of characteristic lifetimes is small, the total curve can be analyzed as follows.

If the rate of photon emission can be expressed as the sum of exponential decay curves,

$$dN/dt = A_1 e^{-t/\tau_1} + A_2 e^{-t/\tau_2} + \ldots\ldots \qquad (11)$$

then the total number of photons emitted following a flash excitation is

$$N = \int_0^\infty (A_1 e^{-t/\tau_1} + A_2 e^{-t/\tau_2} + \ldots\ldots)\,dt \qquad (12)$$

$$= A_1\tau_1 + A_2\tau_2 + \ldots.$$

It is seen that the quantities $A_n\tau_n$ represents the total number of photons emitted by the species corresponding to the lifetime τ_n. The quantities A_n can, in simple cases, be found by extrapolating the decay curve, which gives dN/dt as a function of time, to t = 0. The total number of photons corresponding to each exponential decay can then be obtained from Equation (12) simply by multiplying by the corresponding lifetime, τ_n.

A typical decay curve for RDX_{d-6} is shown in Figure 26. The long tail of the curve is extrapolated back to zero under the assumption that all faster components have died out. The number obtained, A_2, is multiplied by τ_2, obtained from the slope of the straight line, and this product is taken as the total number of photons emitted corresponding to this lifetime. For short times, the difference between the actual curve and the straight line is plotted, and is found to fall on another straight line of different slope, which yields the quantities A_1 and τ_1. The numbers

$$n_1 = A_1\tau_1 / (A_1\tau_1 + A_2\tau_2) \qquad (13)$$

$$n_2 = A_2\tau_2 / (A_1\tau_1 + A_2\tau_2)$$

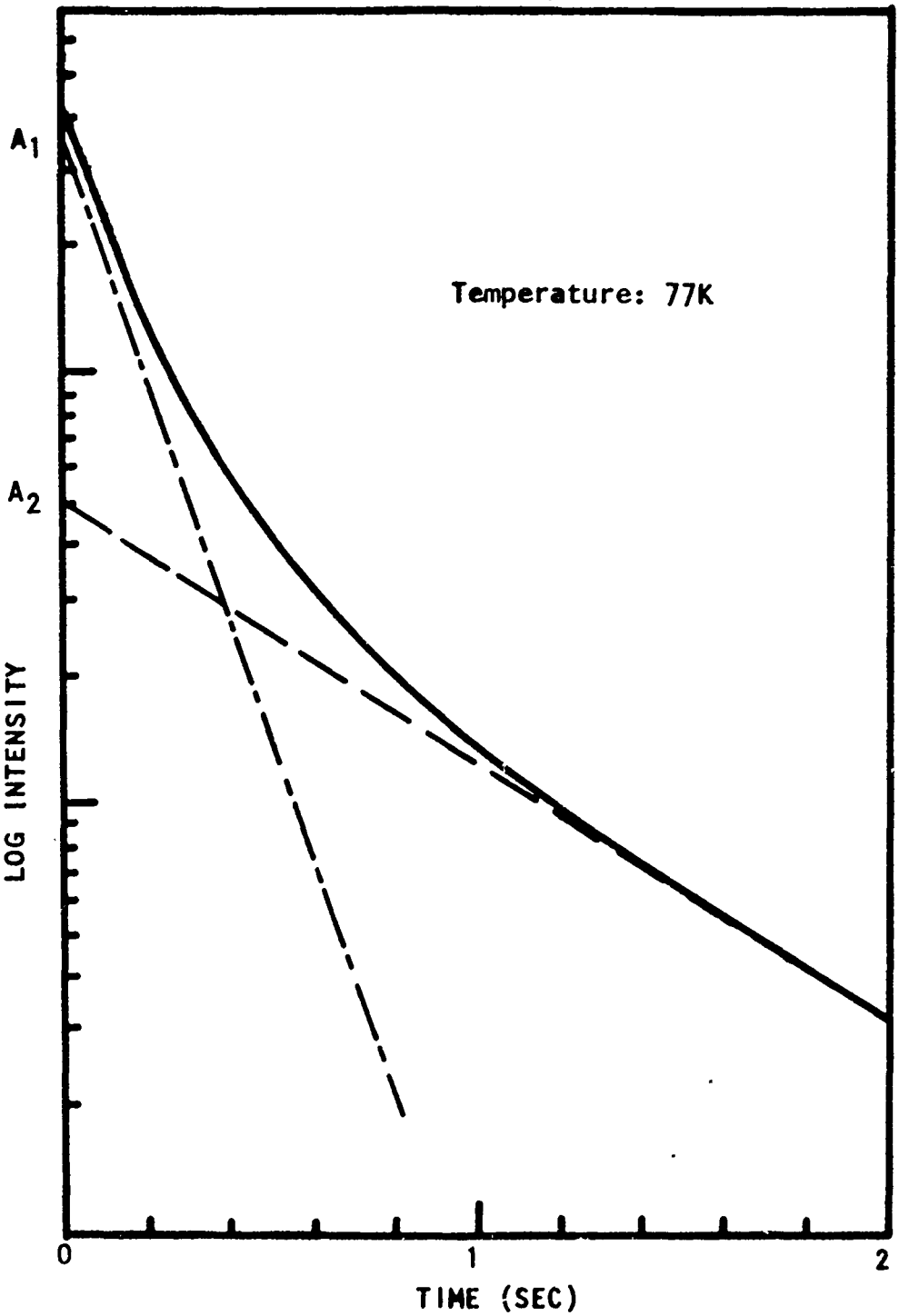

Fig 26 Phosphorescence decay of RDX_{d-6}

represent the fractions of the total emission corresponding to each lifetime. For RDX and HMX the decay curves were well described by the assumption that all A_n were zero for $n > 2$. Table 1 gives the quantities n_1, n_2, τ_1, and τ_2 for both protonated and deuterated RDX and HMX. In all cases, n_1 was of the same order of magnitude as n_2. In all cases, the lifetimes were substantially lengthened as a result of deuteration.

Threshold Wavelength for Photolysis

Powdered samples of both RDX and HMX were irradiated at 77K with progressively shorter wavelengths selected from the output of the 1000-watt xenon arc by the Spectrolab f1.5 grating monochromator used as the excitation monochromator in the luminescence experiments. After one hour of irradiation at a given wavelength, the sample was transferred without warming to a Varian Model V-4500 X-band ESR spectrometer and examined for any signal which might be due to a molecular ion, trapped electron, or free radical. In both materials an ESR signal was observed which resembled that described by Stals (Ref 14) and attributed by him to the NO_2 radical. The cumulative intensity of this ESR signal is plotted in Figure 27 as a function of irradiation wavelength. In both materials no ESR signal is observed when the irradiating wavelength is longer than 340 nm. It has been noted above that this wavelength marks the beginning of a sharp fall-off in the excitation efficiency for both fluorescence and phosphorescence. In addition the threshold appears to correspond with the onset of strong absorption in the nitramine band. Since luminescence can be excited at wavelengths longer than the threshold for photodecomposition, 340 nm can be considered as a boundary separating the luminescence regime from the photodecomposition regime.

Quantum Yields

For purposes of estimating the fluorescence quantum yield of RDX and HMX, an internal standard in the form of guest molecules of Rhodamine-B dye was provided. The fluorescence quantum yield of this substance has been measured (Ref 48) to be 0.97 in ethanol solution. Samples of RDX and HMX were doped with one part per million Rhodamine-B from acetone solution. The fluorescence was then measured at room temperature in an Aminco Bowman spectrofluorometer. When the excitation wavelength was 340 nm, the host fluorescence only was observed. When the excitation wavelength was set at 530 nm, only guest fluorescence was observed, since this wavelength is not absorbed by RDX or HMX.

Table 1

RDX and HMX phosphorescence decay parameters at 77K

	n_1	τ_1 (ms)	n_2	τ_2 (ms)
RDX_{p-6}	.56	120	.44	480
RDX_{d-6}*	.71	160	.29	720
HMX_{p-8}	.65	60	.35	400
HMX_{d-8}*	.44	90	.56	570

* Deuterated samples were kindly supplied by Dr. S. Bulusu of the Explosives Division.

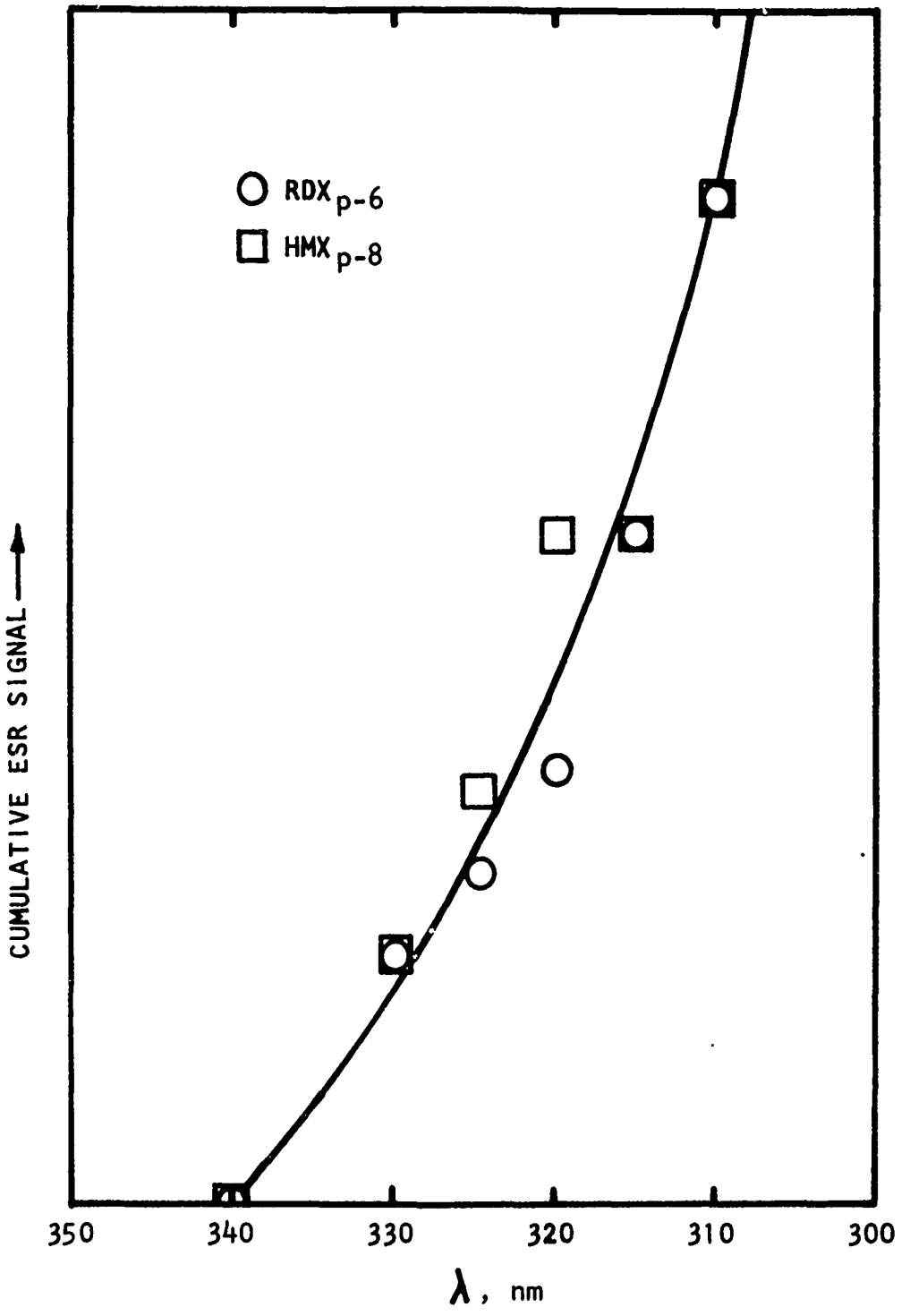

Fig 27 Threshold wavelength for photodecomposition in RDX and HMX

Table 2

Estimated fluorescence and phosphorescence quantum efficiencies for RDX and HMX

	RDX	HMX
Φ_F [1]	10^{-2}—10^{-1}	10^{-2}—10^{-1}
Φ_P [2]	4×10^{-3}—4×10^{-2}	6×10^{-3}—6×10^{-2}
Φ_F/Φ_P [3]	2.4	1.6

Notes:
1. Estimated by comparison with Rhodamine-B fluorescence intensity.
2. Calculated using estimated Φ_F/Φ_P and Φ_F.
3. Estimated from relative fluorescence and phosphorescence intensities.

The assumption is made that the Rhodamine-B fluorescence quantum yield is not changed in going from ethanol solution to RDX or HMX solid solution. There is some justification for this assumption based on the fact that the Rhodamine-B singlet level (2.17 eV) is far removed from the host singlet exciton energy, 3.1 eV. The absorptivity of Rhodamine-B at 530 nm is taken as (Ref 31) equal to 4.6×10^4. It is further assumed that the absorptivities of RDX and HMX at 340 nm are equal to 1, in accordance with the discussion under "Absorption Spectra".

From the fluorescence spectra of the doped samples, the host and guest fluorescence intensities (integrated over the emission spectra) were judged to be approximately equal. The approximate quantum efficiencies of the host materials were then found from

$$\Phi \text{ (Host)} = \Phi \text{ (Rh-B)} \times \frac{\varepsilon \text{ (Rh-B)}}{\varepsilon \text{ (Host)}} \times \frac{[\text{Rh-B}]}{[\text{Host}]} \qquad (14)$$

where Φ (Rh-B) is taken as 0.97, and the ratio of guest to host concentration, [Rh-B]/[Host] is taken as 10^{-6}. The quantity thus obtained, .045, will be modified by factors such as the relative intensities of the excitation at 340 and 530 nm, and therefore only a range of values for the fluorescence quantum yields is given in Table 2.

The ratio of fluorescence to phosphorescence quantum yield was measured using undoped RDX and HMX. The phosphorescence intensity was measured at 77K and 470 nm in the phosphoroscope using an applied photomultiplier voltage of 1200V. The three-window rotating shutter was then replaced with the four-window shutter, and the fluorescence intensity at 300K and 470 nm was measured with 550 V applied to the photomultiplier. This change in tube voltage caused the sensitivity of the system to drop by a factor of 4,368 as subsequently determined by calibration with neutral density filters.

Since the fluorescence is emitted essentially instantaneously, all photons are emitted during the time interval in which the rotating shutter is open. However, for phosphorescence, only a fraction are emitted during this time. This fraction must be known in order to compare the fluorescence and phosphorescence intensities. During the phosphorescence measurements, the speed of the rotating shutter was determined

by displaying the square-wave reference voltage on the oscilloscope. From this information and the dimensions of the shutter, it was estimated that those photons collected were emitted during a time "window" 0.5 ms wide which "opened" 1.25 ms after excitation of the sample. Using the phosphorescence decay parameters for RDX and HMX given in Table 1, it was calculated that the fraction of photons collected was 1/366 for RDX, and 1/172 for HMX.

For purposes of estimating Φ_F/Φ_p the ratios of the fluorescence and phosphorescence spectra integrated over wavelength were taken to be equal to the ratios of the intensities at 470 nm, a wavelength which appears prominently in both fluorescence and phosphorescence. The corrections for the change in PMT voltage and for the fraction of phosphorescence photons passed through the shutter were then applied, and the resulting values for Φ_F/Φ_p are given in Table 2. These values are to be considered only approximate; however the relative value for RDX vs HMX is believed to be meaningful.

The range of values for Φ_p given in Table 2 were calculated from the above ratios of Φ_F/Φ_p and the estimated fluorescence quantum efficiencies.

It should be noted that the quantum yields so obtained are made under the assumption that the quantum yield of the standard, Rhodamine-B, is 0.97 when dissolved in RDX or HMX. In all probability, however, the fluorescence of the standard will be at least partially quenched by the host, causing the true quantum yield to be reduced. This would mean that the fluorescence and phosphorescence quantum yields given in Table 2 for RDX and HMX are probably too large.

DOPED SYSTEMS

Introduction

This section describes the effects of two dopants on the luminescence characteristics of the RDX and HMX hosts. Each dopant is found to influence the host differently, the effects being via (1) complex formation, in the case of anthracene doping; and (2) host-guest energy transfer, in the case of naphthalene doping. The results described are not intended to be definitive studies of these phenomena, as it will be apparent that further study of each effect is warranted. Rather, the results are included for the sake of whatever light they may shed on the properties of the host materials. It is important that the host properties be understood before undertaking studies whose interpretation will depend on those properties. In this regard, the following doping results display the ability of RDX and HMX to form complexes, yield lower bounds to the lowest singlet and triplet state energies of the hosts, and corroborate certain features of the host phosphorescence excitation spectra.

Doping With Anthracene

Acetone solutions of RDX and HMX were doped with anthracene (99.999% pure, obtained from Princeton Organics, Inc.) in an amount sufficient to yield a mole ratio of about 500 parts anthracene to 10^6 parts RDX or HMX. The solutions were kept in the dark as the solvent was evaporated. The solid was transferred to the phosphoroscope without exposure to light and yielded the phosphorescence spectrum indicated by the dashed line in Figure 28. This is the phosphorescence spectrum displayed by undoped RDX or HMX.

The sample was subsequently exposed to room light at room temperature for about 24 hours, after which it was again examined in the phosphoroscope. The phosphorescence was now several times more intense and showed resolved vibrational structure (solid line in Figure 28). The vibrational interval is approximately 1600 cm^{-1}, and what appears to be the 0-0 transition lies at 453 nm. The phosphorescence excitation is also shown in Figure 28, where it is compared with that of undoped material. Here, too, vibrational structure is observed, with new bands seen at approximately 360, 377, and 407 nm. To the short-wavelength side of these bands, which are not characteristic of the HMX

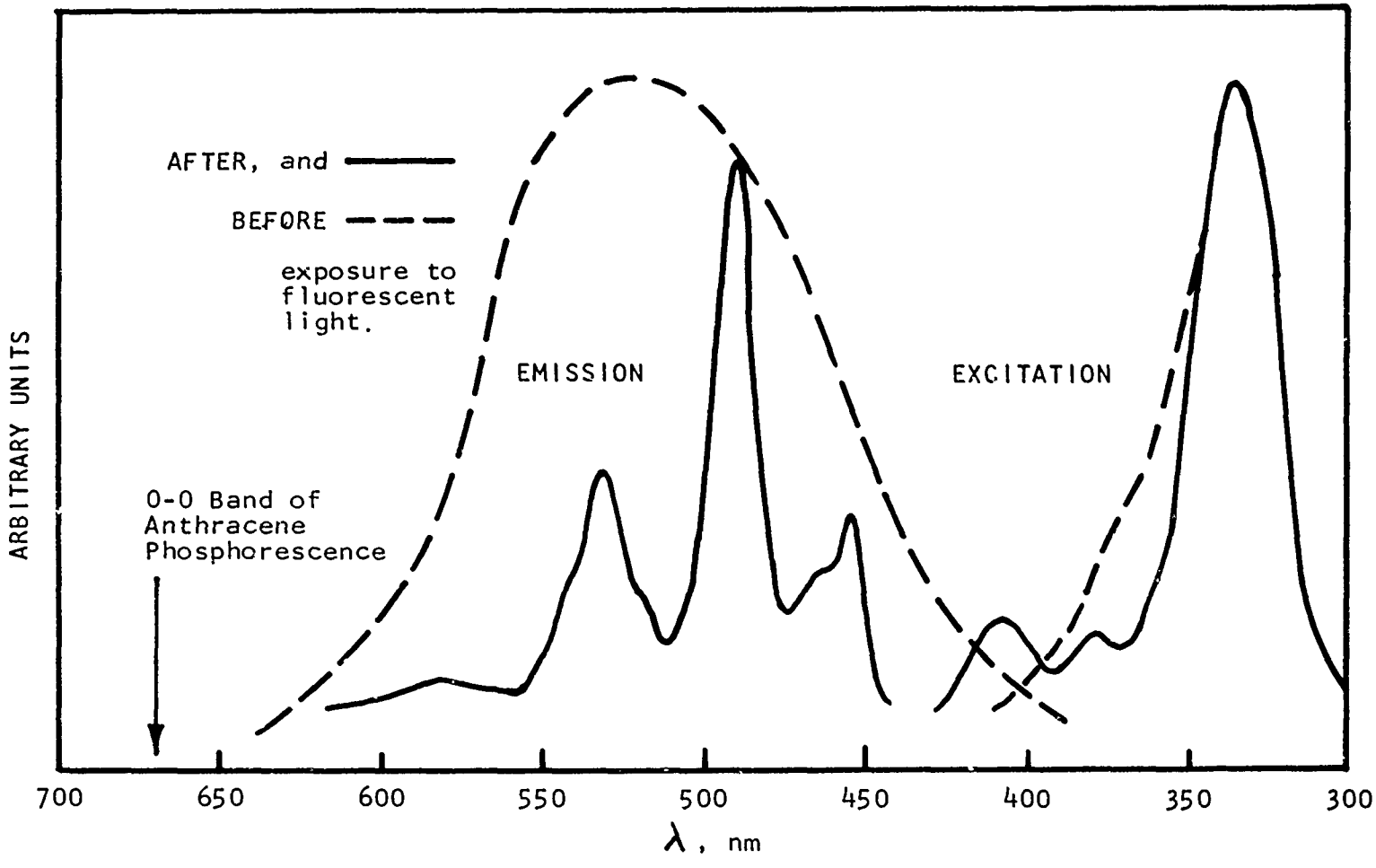

Fig 28 Phosphorescence and phosphorescence excitation spectra of HMX doped with anthracene

host, is the main phosphorescence excitation peak at 340 nm, in exact agreement with that of undoped HMX.

The fluorescence of the samples is quite intense, and appears blue to the eye. The fluorescence spectrum is shown in Figure 29, where it can be seen that neither the peak positions nor the vibrational interval of about 1400 cm^{-1} correspond to those in the phosphorescence spectrum. Therefore there is no possibility that the structured phosphorescence of the anthracene-doped HMX is due to anthracene fluorescence which is somehow red-shifted to longer wavelengths.

It will be noted that from Figures 28 and 29 excitation at 340 nm produces relatively more phosphorescence than fluorescence. This may be due to the fact that irradiation at this wavelength would primarily excite the host HMX molecules. Because of the presence of four nitro groups per HMX molecule, intersystem crossing is expected to be rapid, and fluorescence may be partially quenched, with a corresponding enhancement of phosphorescence.

It seems clear from the fact that exposure to light is necessary for the appearance of the structured phosphorescence spectrum that a photocomplex between an anthracene and a host molecule is formed under the action of light. Although anthracene is known to form photodimers, especially in solution (Ref 32), the fact that these doped samples were grown in the dark argues against such species being responsible for the structured phosphorescence. In addition, phosphorescence from an anthracene photodimer is expected to be red shifted from that of the monomer, and to be even farther removed from the observed emission.

Crystals of an RDX-Anthracene photocomplex were successfully isolated by evaporating the solvent from a solution containing equimolar amounts of RDX and anthracene light. Evaporation under incandescent light or in the dark produced crystals of the two separate components, which could be identified by their melting points. Crystals of the photocomplex melted at about 192°C, as compared with 203°C for pure RDX and 217°C for pure anthracene. Preliminary elemental analysis was performed by Schwartzkopf Microanalytical Laboratory of Woodside, New York. The results are presented in Table 3, and are seen to be in fair agreement with the assumption of a 1:1 complex. However, it is quite possible that there could be an excess of anthracene in the crystals. Any uncomplexed anthracene would be expected to have an effect on the luminescence, and particularly the fluorescence properties.

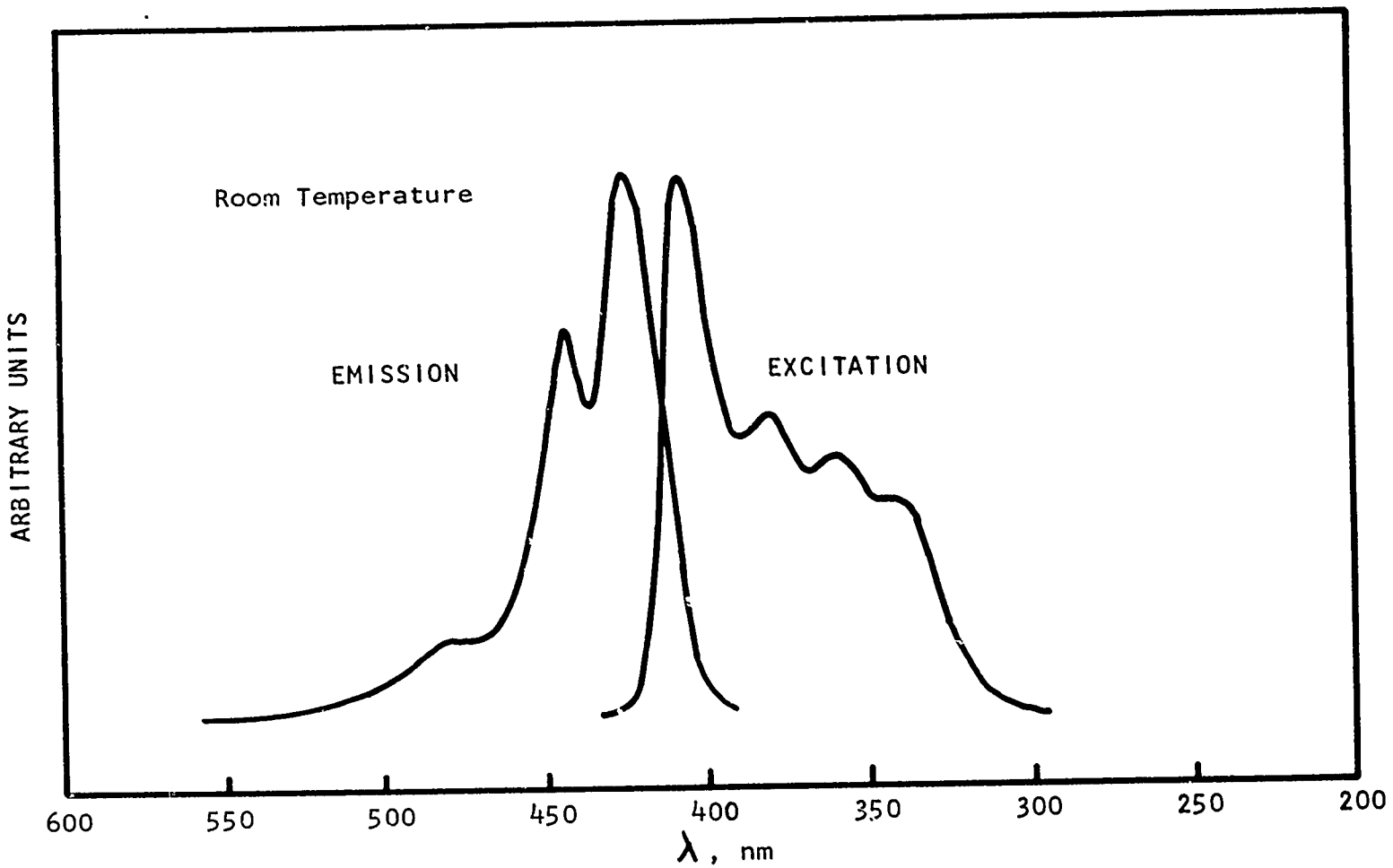

Fig 29 Fluorescence and fluorescence excitation spectra of HMX doped with anthracene

Table 3

Results of carbon, nitrogen, and hydrogen analysis of RDX-anthracene complex*

	Run #1	Run #2	Run #3	Calculated for 1:1 Complex
C	65.4%	59.0%	57.7%	51%
N	27.6%	21.6%	21.5%	21%
H	4.6%	4.2%	3.3%	4%

* Analysis performed by Schwartzkopf Microanalytical Laboratory, Woodside, NY

NMR spectra of crystals of the RDX-Anthracene complex dissolved in deuterated acetone were a superposition of the spectra of RDX and anthracene separately. This indicates that neither of the two components is destroyed by the complexation.

As shown in Figure 30, the phosphorescence spectrum of the complex crystals is nearly identical to that of the anthracene-doped HMX. However, the phosphorescence excitation spectrum shows the main peak somewhat shifted to the blue, at 335 nm. This is no doubt because the RDX which is responsible for this peak is diluted by the presence of an equimolar amount of anthracene, allowing shorter wavelengths to penetrate the crystal. In addition, some structure is observed near 285 and 310 nm. It should be noted that the absorption spectra of RDX and HMX thin films also show structure at these wavelengths.

The fluorescence and fluorescence excitation spectra for the complex crystals are shown in Figure 31. They are similar to those of the anthracene-doped HMX. The absorption spectrum of the crystal is also shown, and is seen to display a shoulder near 407 nm. The presence of this band in the absorption and luminescence excitation spectra may indicate a charge-transfer nature for the complex. If this were the case, it would be easy to understand how the presence of the anthracene dopant in an RDX or HMX host can so enhance the phosphorescence intensity. This band, lying at longer wavelengths than the absorption due to the host (or guest) corresponds to a trapping level at lower energy than the host singlet exciton band. Thus, energy absorbed by the host crystal is funnelled into the localized energy levels of an RDX-Anthracene complex dopant. By intersystem crossing it eventually finds itself in the lowest triplet state of the complex, which is also expected to lie lower in energy than the host triplet exciton band. Thus, the funnelled energy is eventually reradiated as phosphorescence.

Since RDX or HMX in solution does not absorb appreciably at wavelengths longer than about 350 nm (Fig 14 and 15), and since anthracene in solution absorbs to about 390 nm, it seems likely that during the growth of the complex crystals it is the anthracene which is excited by the floures-cent light. The complexation reaction may proceed by

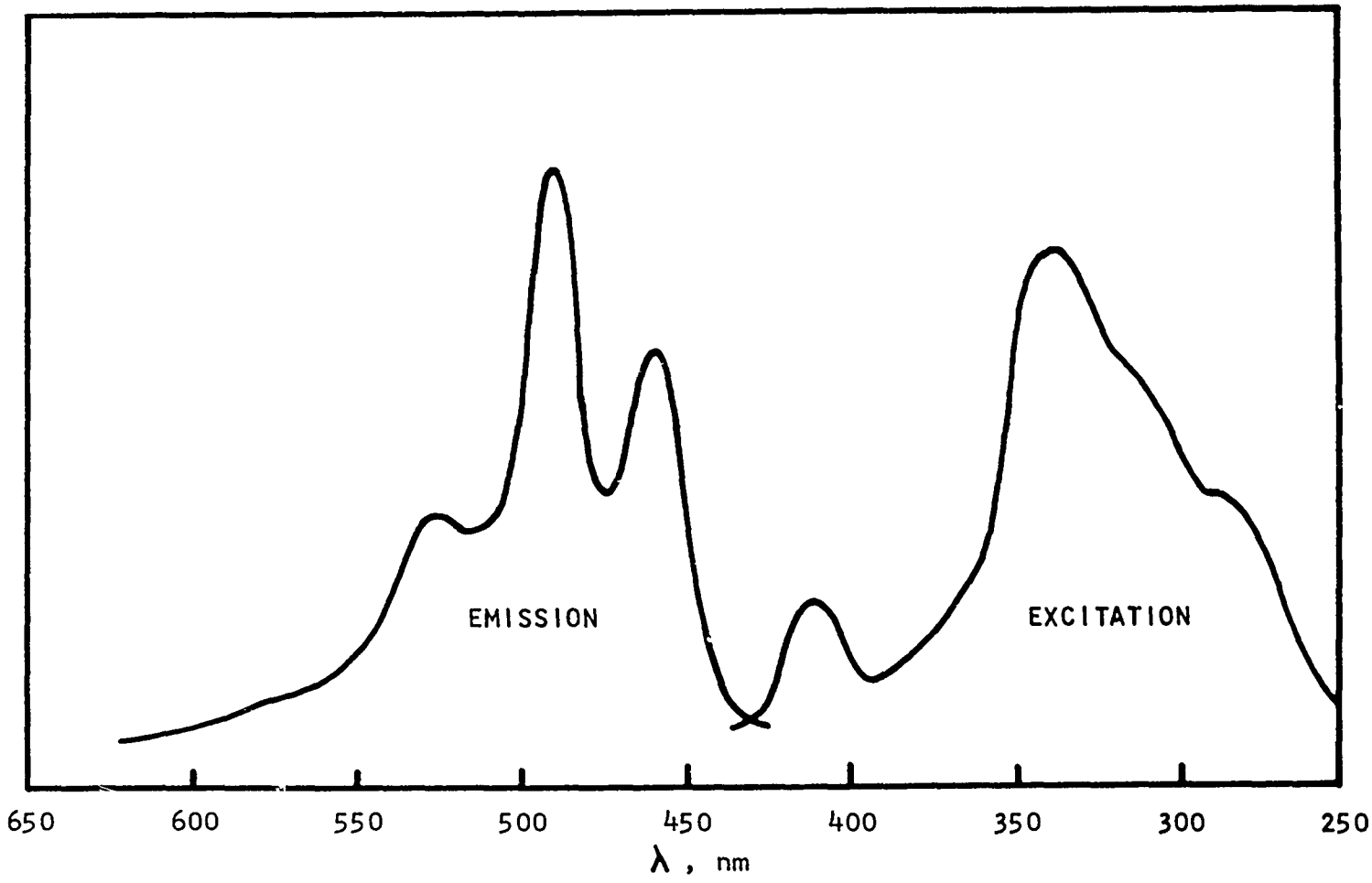

Fig 30 Phosphorescence and phosphorescence excitation of RDX-Anthracene single crystal

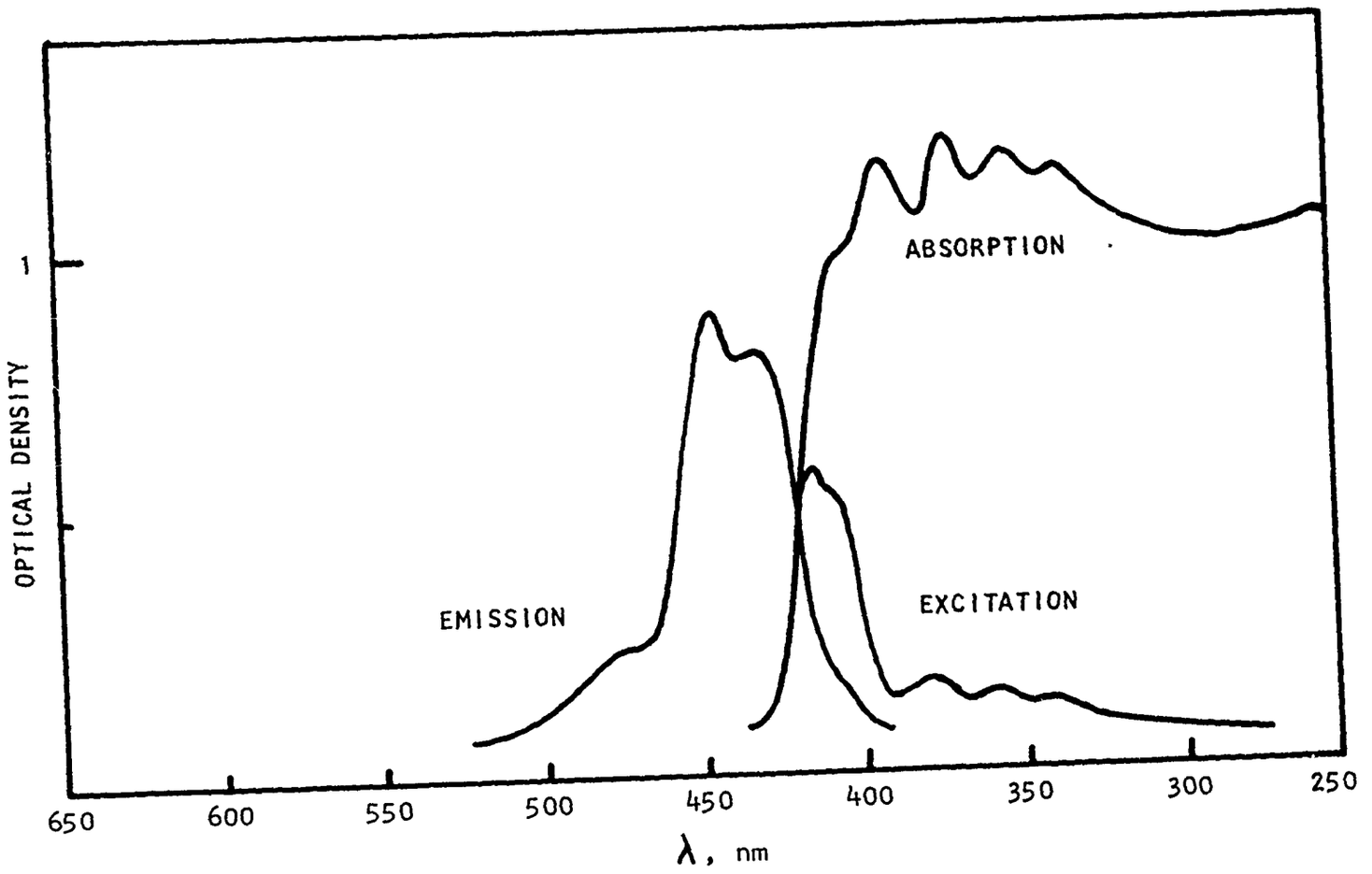

Fig 31 Fluorescence and fluorescence excitation of RDX-anthracene single crystal

$$RDX + Ant + h\nu \rightarrow RDX + Ant^*$$

$$\rightarrow (RDX\text{-}Ant)^*$$

$$\rightarrow (RDX\text{-}Ant) + h\nu'$$

It is known that electronically excited molecules have a greater electron affinity than those in the ground state (Ref 33). Thus, excitation can produce charge-transfer reactions which lead to excited charge-transfer complexes. This implies that if indeed the RDX-Anthracene complex is formed subsequent to excitation of the anthracene molecule, it is the RDX which is the donor and anthracene the acceptor. This is consistent with the experimentally observed fact that the phosphorescence of a charge-transfer complex usually consists of donor phosphorescence (Ref 1). We have seen above that the structured phosphorescence of the complex cannot be attributed to anthracene; if it is donor phosphorescence, then RDX must be the donor. In addition, if the structured phosphorescence is attributable to the RDX donor, it helps explain the fact that the phosphorescence of undoped RDX or HMX is approximately the envelope of the structured complex phosphorescence.

It was stated above that the increase in phosphorescence intensity due to complex formation is probably due to trapping of excitation energy at the dopant site. This implies that the host triplet exciton band lies higher in energy than the triplet energy level of the complex, which from Figure 28 we may estimate as 2.7 eV. This number is obtained by noting that the apparent 0-0 band of the complex phosphorescence lies at a wavelength of 453 nm, corresponding to the above energy.

Doping with Naphthalene

Samples of HMX were doped with about 1000 parts per million naphthalene (99.999% pure, obtained from Princeton Organics, Inc.). Napththalene phosphorescence occurs at about the same wavelengths as that of undoped HMX, and so the resultant phosphorescence spectrum is similar to that of undoped HMX. However, features due to the naphthalene guest are discernible at 460, 505, and 550 nm in the spectrum of Figure 32 which shows the phosphorescence from naphthalene-doped HMX. The intensity of the phosphorescence was much greater than for an undoped sample. Phosphorescence decay was measured through a Corning

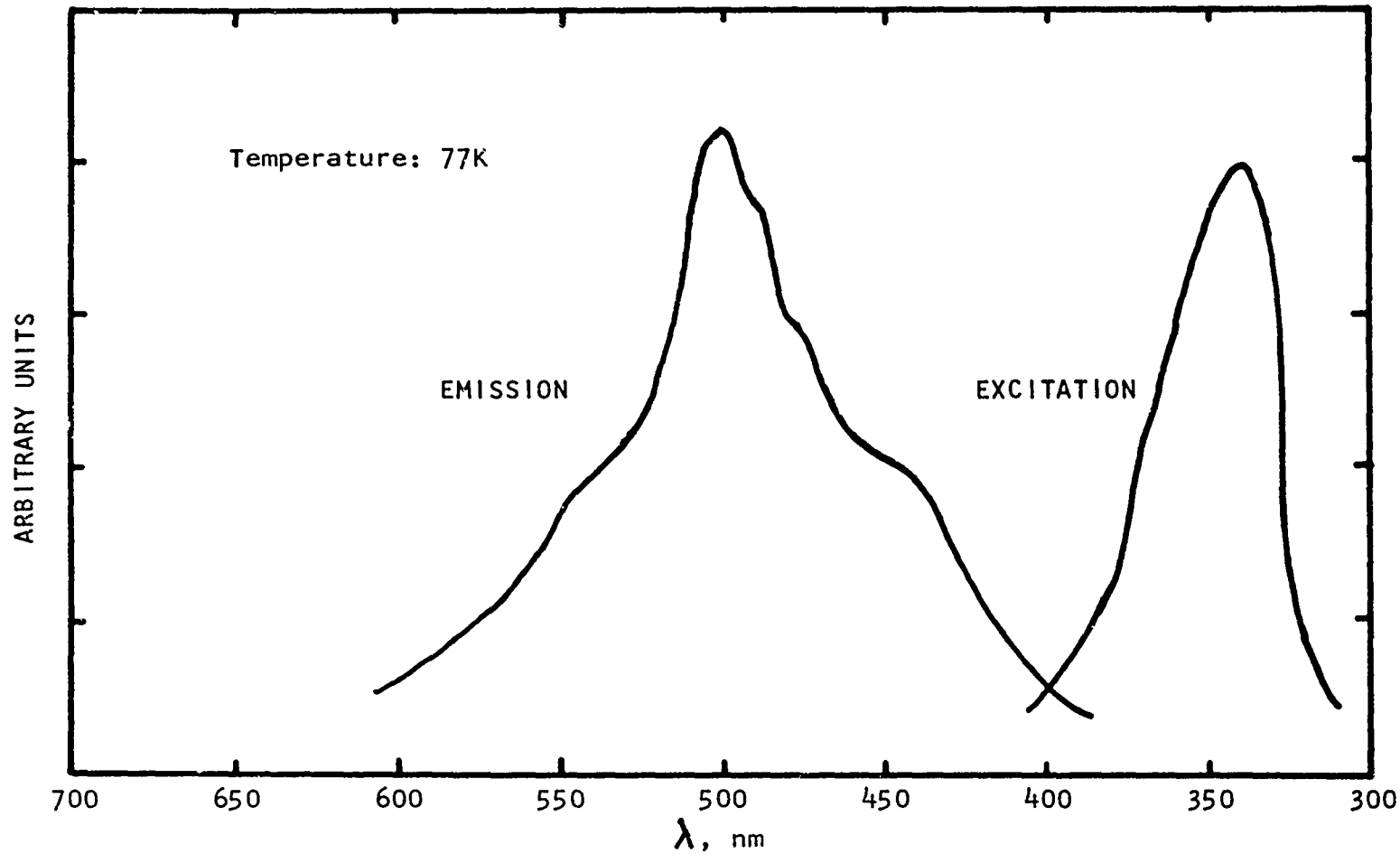

Fig 32 Phosphorescence and phosphorescence excitation of naphthalene-doped HMX

No. 3-71 glass color filter, which passes wavelengths longer than about 465 nm. The results are shown in Figure 33 where it is seen that there is an initial nonexponential decay, followed by an exponential tail corresponding to a lifetime of about 580 ms. This lifetime is too long, and the emission too bright to be due to the HMX host, and is thus attributed to the naphthalene guest.

It was noted in the Introduction that naphthalene in solution is transparent at wavelengths longer than about 310 nm, and this is also true of the naphthalene crystal. Thus, the naphthalene guest, whether it enters the HMX crystal as individual molecules or some form of aggregate, cannot account for the fact that naphthalene emission is observed when the doped HMX is excited at wavelengths longer than 310 nm. Indeed, it is seen that in Figure 32 the phosphorescence excitation spectrum is identical with that of undoped HMX. It is clear that the naphthalene guest cannot be absorbing excitation energy directly from the exciting light, and must therefore be the acceptor in some energy transfer process.

Since the naphthalene singlet state lies at about 4 eV, higher in energy than the incident photons, the only possible way in which the guest singlet state could be excited is by triplet-triplet annihilation of host excitons. Excitation of the guest triplet state could be via excitonic transfer, resonance transfer or some other short range process.

Using the fact that the density of solid HMX is 1.9 g/cc, and its molecular weight being 296, one can calculate that solid HMX has 3.87×10^{21} molecules per cubic centimeter. If one in one thousand of these is a naphthalene guest, then there are 3.87×10^{18} guest molecules per cc, and the average volume per guest molecule is 2.58×10^{-19} cc. This corresponds to a sphere of radius 43 Å, and thus the average center-to-center distance between guest molecules is 86 Å. Thus, if the excitation of the HMX molecules is random, the energy would need to travel up to 43 Å before transferring to a guest molecule. This seems too large a distance to be consistent with the Föerster resonance transfer mechanism, particularly since the required transitions in both donor and acceptor molecules are forbidden. Singlet excitons are too short-lived to carry energy this distance and it appears that triplet excitons may be responsible.

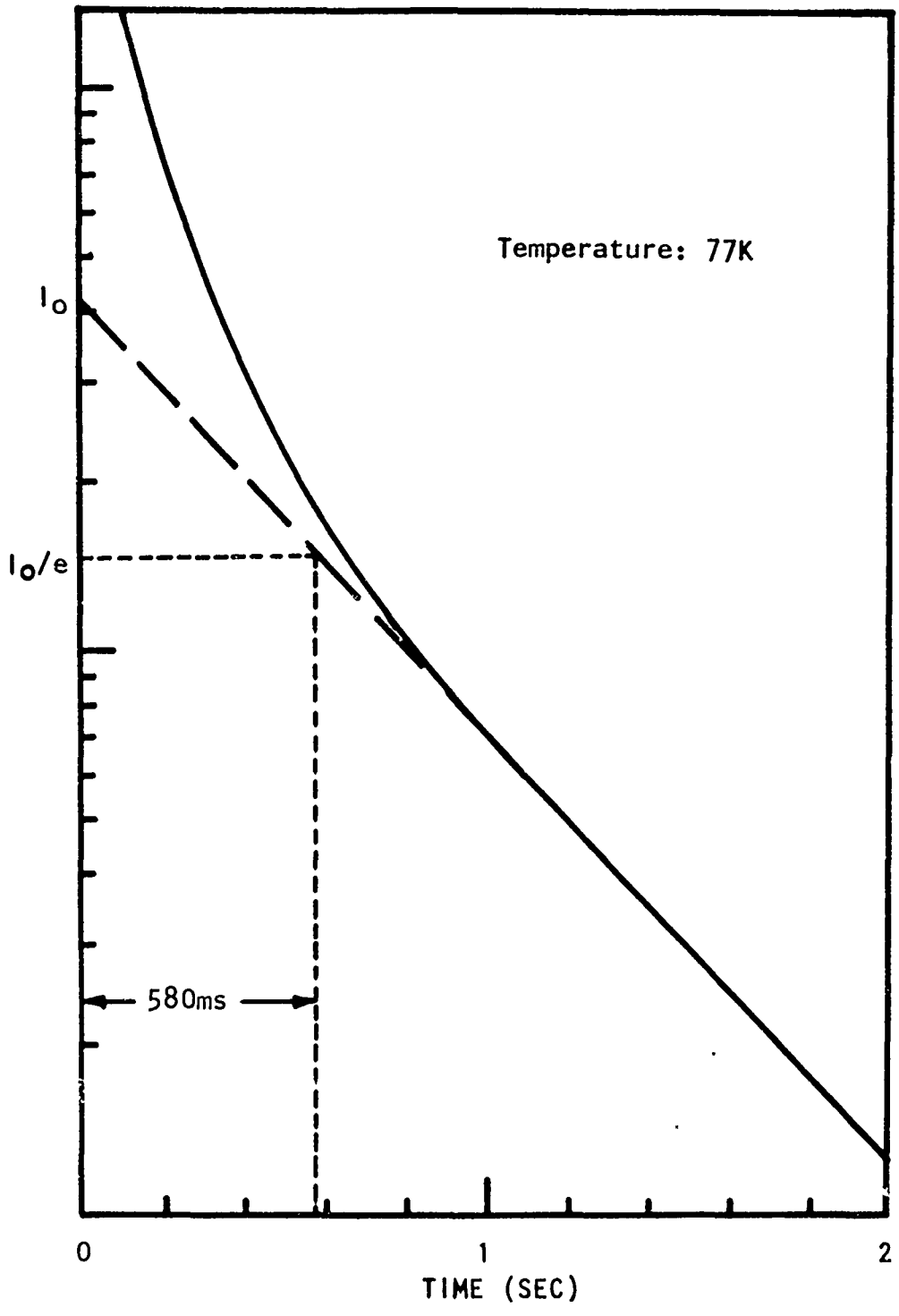

Fig 33 Phosphorescence decay of HMX: naphthalene

DISCUSSION

The Evidence for Triplet Luminescence

It is conceivable that mechanisms other than emission from a molecular triplet state could account for the long-lived luminescence from RDX and HMX. Irradiation with ultraviolet light could cause trapping of electrons, which could recombine slowly with their donors, yielding a long-lived recombination luminescence. Since both the donor and the trapped electron are expected to be paramagnetic, they should be detectable by ESR.

Therefore samples of solid RDX and HMX were examined in a Varian Model V-4500 ESR spectrometer at a microwave frequency of 9.5 GHz (X-band) and at liquid nitrogen temperature (77K), while under irradiation with 340 nm light. This wavelength corresponds to the peak of the fluorescence and phosphorescence excitation spectra, and should be the most efficient wavelength for producing a trapped electron population. No signals were observed which could be attributed to trapped electrons or free radicals. Thus, it is concluded that recombination luminescence is not responsible for the emissions observed in RDX and HMX.

Furthermore, no ESR signals were observed after cessation of irradiation with 340 nm light. This is consistent with the findings reported at the end of section entitled Characterization of Undoped RDX and HMX, to the effect that the threshold decomposition wavelength as determined by the appearance of the NO_2 radical ESR signal is $\lambda<340$ nm, to the short wavelength side of the luminescence excitation peak. From these observations it is not considered likely that the luminescences are due either to charge separation, or to decomposition products.

Further evidence against a charge separation origin for the luminescences is found in the results of photoconductivity experiments on single crystals of RDX and HMX (Ref 34). Here it is found that at 77K these materials exhibit no conductivity for wavelengths longer than about 275 nm. This threshold is well removed from the luminescence excitation peak, and indeed is in the region where photolytic decomposition is known to occur.

It is shown in Table 1 of section entitled Characterization of Undoped RDX and HMX that deuteration of RDX and HMX leads to substantially lengthened phosphorescence lifetimes. This is a general phenomenon which is due to a smaller nonradiative transition probability for the deuterated analogs relative to the protonated compounds (Ref 1). Unless the effect in RDX and HMX is caused by deuteration of an impurity during the synthetic process, the evidence of Table 1 indicates a triplet state origin for the phosphorescence.

The measured phosphorescence lifetimes for both the protonated and deuterated materials are also in accord with the known effect of the nitro substituent on the triplet state lifetimes (Ref 3), as described in section entitled Characterization of Undoped RDX and HMX. There it was noted that each nitro group is expected to act as a spin-orbit coupling center, thereby reducing the phosphorescence lifetime. Since HMX has four such centers and RDX only three, one might expect a shorter phosphorescence lifetime for the former. It is seen from the data in Table 1 that this is indeed the case.

It is seen from Table 2 that the ratio of fluorescence quantum efficiency to that of phosphorescence is greater in RDX than in HMX. This fact is understandable in terms of the enhanced intersystem crossing rate expected in the compound with the greater number of nitro groups. The greater this rate, the more the fluorescence is expected to be quenched.

The Impurity Question

Spurious results from unintentional impurities are always a hazard in luminescence spectroscopy. Tiny quantities of a luminescent impurity can completely swamp the intrinsic luminescence of a material under study. As we have seen, zone refining is not applicable to RDX or HMX, because they decompose at their melting points. Therefore, purification of the materials used in this work rests on recrystallization from spectrograde solvents a minimum of five times. For HMX, snythesis by nitrolysis of DADN, which is an eight-membered ring compound, reduces the chance of contamination by RDX. However, since the measured results for the two compounds are virtually identical, this is believed to be of little consequence.

NMR spectra of the recrystallized materials showed no trace of impurity, although the sensitivity of this method is such that one does not expect to detect impurities present in concentrations less than about 1%.

The likely impurities in RDX and HMX are compounds which have been isolated in the study of methods for the manufacture of these explosives. The chemistry of these compounds has been described by Bachmann and Sheehan (Ref 35), and Wright, et al, (Ref 36). The ultraviolet absorption spectra of these compounds show no absorption at 340 nm (Ref 37). Some of them are water soluble and can be easily removed by washing the freshly synthesized RDX or HMX with hot water.

Other conceivable impurities are compounds containing the nitroso (NO) group. The presence of this group in a molecule causes the appearance of weak ($\varepsilon \approx 100$) absorption at 360 to 385 nm (Ref 38). This is in the vicinity of the absorption seen in solid RDX and HMX; however, nitroso compounds are not known to be luminescent, and could not be responsible for the excitation of fluorescence and phosphorescence near 340 nm.

In saturated molecules such as RDX and HMX, the presence of the nitro group is not known to cause the appearance of an absorption band near 340 nm. However, the class of nitroaromatic compounds is expected to display a weak ($\varepsilon \approx 100$) absorption near 350 nm (Ref 39). However, it is difficult to imagine how an aromatic compound could be synthesized under the conditions which prevail in RDX and HMX synthesis.

In addition to the above considerations, the fact that a band at 340 nm is not observed in solvated RDX or HMX seems to argue that an impurity is not responsible, since its absorption should not disappear in solution. Since the luminescence excitation occurs at the same wavelength as the band observed in the solid materials, the implication is that the luminescence is intrinsic.

The phosphorescence excitation spectrum of naphthalene-doped HMX reproduces that of the undoped material, and again corresponds to the 340 nm absorption band. This suggests very strongly that the naphthalene guest acquires its energy from the HMX host. If the energy were received instead from an impurity, X, having its singlet-singlet absorption at 340 nm, then radiative transfer to the naphthalene could be ruled out by the fact that X could only fluoresce at $\lambda \geq 340$ nm, where naphthalene absorption is nonexistent. Reassignment of the 340 nm band to an impurity means raising our estimates of the host singlet and triplet exciton bands in accordance with the calculations of Orloff, et al, (Ref 5). Thus, transfer of energy from X to naphthalene through a host exciton band would require thermal energy greater than that available at the measurement temperature, 77K. And finally, transfer via short-range processes such as resonance transfer is rendered unlikely by the low probability of finding the two types of guest molecules close together.

The Nature of the Absorbing Species

The absorption band shown in Figures 9 and 10 is in excellent agreement with the fluorescence excitation spectra of the corresponding samples shown in Figures 17 and 19 with regard to shape and peak position. Since neither absorption nor fluorescence excitation in this band is observed for solvated RDX or HMX, it could therefore be attributed to either (1) a Davydov component of the nitramine band, or (2) charge-transfer absorption.

The Davydov interaction splits a transition into several components, the number depending on the number of molecules per unit cell. In many cases the lowest energy transition is forbidden (Ref 40), and not observable in absorption. In RDX and HMX crystals there are eight and two molecules per unit cell, respectively, so that such a Davydov splitting is possible, and could account for the low intensity of the 340 nm band. The magnitude of Davydov splitting depends on the strength of the transition in the isolated molecule, and is thus dependant on the molar absorptivity. Only in the case of the strongest transitions, such as the 250 nm system in anthracene where $\varepsilon = 40,000$ $M^{-1}cm^{-1}$ does this splitting approach 14,000 cm^{-1} (Ref 32). In the isolated RDX molecule, the nitramine band has a molar absorptivity of 11,000 and the 340 nm band is red shifted from the position of the

nitramine band in the solid by 12000 cm^{-1}. Stals (Ref 27) has estimated the expected splitting in RDX as 2000 cm^{-1}, making this an unlikely explanation for the 340 nm band.

Charge-transfer dimers have been found to form in concentrated solutions of certain compounds (Ref 41). The formation of these entities leads to a new absorption band at longer wavelengths than the monomer absorption. In addition there is fluorescence excitation corresponding to this band, which occurs at 350 nm. The fluorescence emission is a structureless band which peaks at 450 nm. It is possible to imagine an entire crystal bound by such charge-transfer forces, i.e., a charge-transfer aggregate. In such an aggregate, the charge-transfer band of the dimer would be replaced by a band characteristic of the crystal as a whole. This band would be expected to lie at longer wavelengths than the monomer absorption, and excitation within it would be expected to give rise to charge-transfer fluorescence and phosphorescence. Luminescences from charge-transfer complexes normally consist of broad bands devoid of structure, with a good deal of overlap between the fluorescence and phosphorescence bands (Ref 21). These characteristics are observed in the RDX and HMX luminescence spectra of Figures 17-25.

Stals (Ref 27) has noted that charge-transfer bands normally lie above the first singlet exciton band (Ref 19). This is true for such bands in the nonpolar aromatics, where it is due to the lack of polarization energy to assist in the charge transfer. However, RDX and HMX are highly polar molecules, and it is thus not unreasonable that in these materials a charge-transfer band be lower in energy than the first singlet exciton band.

Charge-transfer bands are ordinarily quite intense, and molar absorptivity in the vicinity of 15,000 M^{-1} cm^{-1} is common. However, measurements (Ref 42) on the charge-transfer complex formed between boron trifluoride (a strong electron acceptor) and hexamethylene tetramine (the starting material for synthesis of RDX and HMX) show the charge-transfer band to have a molar absorptivity of only two. This is comparable in intensity to the value measured in RDX and HMX crystals at 340 nm. Thus, it may be that charge-transfer bands in these materials are anomalously weak. The absorption, fluorescence, and phosphorescence spectra of this complex are similar to those of RDX and HMX, but shifted to shorter wavelengths, and the charge-transfer absorption lies lower in energy than the first singlet exciton band of the uncomplexed hexamethylene-tetramine.

The fact that absorption in the range 320-420 nm appears more prominently in the reflectance and thin-film spectra suggests that it is connected with entities near the surface of the crystal, perhaps at or by defects. If the charge-transfer band is anomalously weak because of some selection rule, absorption might take place primarily near defect sites where the lower site symmetry breaks that selection rule.

The Nature of the Luminescent Species

The broad, unstructured fluorescence and phosphorescence bands are consistent with either (1) excimer or (2) complex luminescence. It will be recalled from the discussion of section entitled Introduction that an excimer has no stable ground state, and that aggregation does not occur until a monomeric molecule is excited by an incident photon. Therefore, in the case of excimer luminescence, the absorption and luminescence excitation spectra correspond to those of the monomer. This is not the case for RDX and HMX, where the absorption and excitation spectra of the solid differ from those of the isolated molecule.

We are thus led back to the suggestion of Stals that charge-transfer self-complexation occurs when RDX and HMX crystallize. Although this hypothesis was made on the basis of absorption data, it is also consistent with the unstructured luminescences and the large degree of overlap between the fluorescence and phosphorescence. The absorption data suggest that defects play a role in the absorption of incident light. Defects are also expected to act as traps for excitation energy in a crystal. Photodimerization of anthracene is known to take place preferentially at defect sites (Ref 43), and defect fluorescence has been reported by Helfrich and Lipsett (Ref 44). Nonuniformity of the defect sites could explain the nonexponential phosphorescence decay measured in RDX and HMX, particularly in view of the fact that these materials both have alternate crystal structures. It is possible to imagine that the defect sites are submicroscopic regions in which the molecular ordering differs from the rest of the crystal.

It is considered significant that the fluorescence and phosphorescence excitation efficiencies drop sharply at 340 nm, the wavelength at which solutions and thin single crystals begin to absorb strongly. The strong absorption is taken to be characteristic of the monomer, excitation of which is believed to lead to dissociation of the molecule rather than reemission of a photon. This interpretation is supported

by the calculations of Stals (Ref 27), who concludes that both the lowest excited singlet and triplet states of the nitramine group are expected to undergo C-N bond cleavages. In addition, the threshold for photodecomposition as discussed in section entitled Characterization of Undoped RDX and HMX was found to lie at 340 nm, corresponding to the sharp drop in luminescence efficiency. The situation is diagrammed in Figure 34. At wavelengths shorter than 340 nm, the molecules are excited to the singlet exciton band derived from states of the isolated molecule, leading to photodecomposition rather than luminescence. At longer wavelengths, excitation is to the charge-transfer singlet exciton band, leading to luminescence.

Estimated Singlet and Triplet State Energies

The fact that HMX can transfer energy to a naphthalene guest molecule, whatever the mechanism, allows a lower bond to be placed on the triplet state of the donor, since, by conservation of energy, it must be larger than that of the naphthalene acceptor. This means that $E_T \geq 2.64$ eV. Similarly, the phosphorescence of the HMX-anthracene complex is more intense than that of the HMX host, indicating that the complex triplet level functions as a trap, and is thus lower in energy than the host triplet exciton band. From the discussion in section entitled Doped Systems, this means that $E_T \geq 2.74$ eV. Finally, from the HMX phosphorescence spectrum of Figure 24 we may estimate that the 0-0 band, were it resolved, would lie near 450 nm, corresponding to an energy of 2.76 eV. These three estimates are all in substantial agreement.

In section entitled Doped Systems it was noted that a new absorption and excitation band appears when HMX complexes with anthracene. If, as expected, this new charge-transfer band occurs at lower energy than the host singlet esciton band, a lower bound is placed on the host singlet exciton band energy: $E_S \geq 3.05$ eV. Also, from the fluorescence excitation spectra, the host singlet exciton band energy was estimated in section entitled Characterization of RDX and HMX to be 3.1 eV, in substantial agreement.

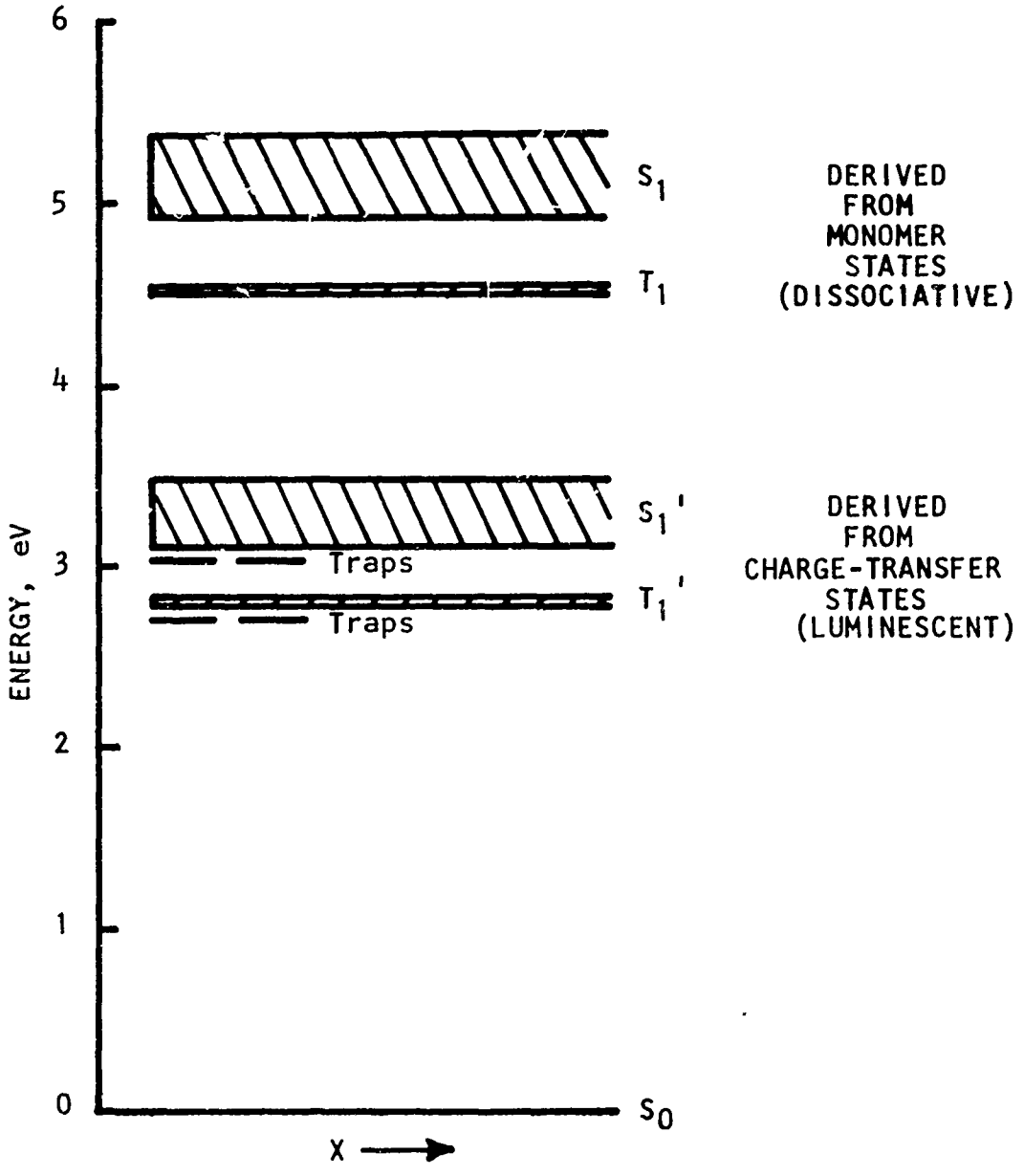

Fig 34 Proposed band structure of solid RDX and HMX

The above estimates lead to a singlet-triplet splitting of approximately 0.35 eV. This is a rather small value, as indeed it should be for a nonaromatic molecule such as RDX or HMX. In addition, the postulated charge-transfer nature of the emitting species requires a small singlet-triplet splitting.

The molecular orbital calculations of Stals (Ref 45) indicate that the equatorial nitramine group of both RDX and HMX should have a $1\,^3B_2$ triplet state with an energy of 2.76 eV. This value is in excellent agreement with that estimated above from the phosphorescence measurements. Thus, it is possible that the lowest triplet state in solid RDX and HMX is derived from a monomeric state, rather than from a charge-transfer dimeric one. However, the same calculations indicate that this state should be dissociative rather than luminescent.

SUMMARY

This work reports for the first time the observation of both fluorescence and phosphorescence from the cyclic polynitramines known as RDX and HMX. Luminescent emission has not previously been observed from this class of compounds. The excitation spectra for both fluorescence and phosphorescence have been shown to correspond to a weak absorption band which is observed in the solid, but not in the solvated state. The emission spectra are broad bands devoid of vibrational structure, from which the rather small value of approximately 0.35 eV is deduced for the singlet-triplet splitting. There is a definite effect of deuteration on long-phosphorescence lifetimes, signifying a triplet state origin for the long lived emission. The phosphorescence decay is found to be nonexponential, and to have no component due to thermally-stimulated fluorescence. The phosphorescence decay is found to be faster for HMX than for RDX, in accordance with expectations based on the known effect of the nitro substituent on triplet state lifetimes. The threshold wavelength for photolysis was measured and found to coincide with a steep drop in the efficiency of luminescence excitation. Doping experiments with energy acceptors have allowed the estimation of the singlet and triplet state energies as 3.1 and 1.75 eV, respectively.

Because the weak absorption band appears upon crystallization, and because the required Davydov splitting would be much too large, it is interpreted as being due to charge-transfer self-complexation. This assignment is consistent with the known tendency of these materials to form crystals in which the bonding is primarily electrostatic in nature, as inferred from crystallographic studies. The fact that the band is more distinct in measurements involving reflection from a single crystal surface, and in transmission measurements on thin films suggests that crystal defects may play a role.

The characteristics of the luminescent emissions are also consistent with those expected from a charge-transfer complex, i.e., broad, structureless bands with considerable overlap between fluorescence and phosphorescence, indicative of a small singlet-triplet splitting. The estimated triplet state energy (2.75 eV) is in exact agreement with that calculated for the equatorial nitramine groups of RDX and HMX, and so a localized triplet excited state rather than a charge-transfer state cannot be ruled out. However, the same calculations predict that the molecular triplet should be dissociative, and thus non-luminescent.

The sharp drop in luminescence excitation efficiency at wavelengths shorter than 340 nm is interpreted as due to excitation of non-luminescent states of the isolated molecule. This interpretation is consistent with the onset of photodecomposition detected by ESR at this wavelength.

The model postulated to explain the experimental results assumes two types of singlet and triplet exciton bands: those derived from monomeric states, nonluminescent, and having energies comparable to those of the monomeric states; and those derived from charge-transfer dimer states, luminescent, and occurring at lower energies. The occurrence of new absorptions (aside from those due to Davydov splitting) has no parallel in the aromatic solids, in which the bonding in the solid is due primarily to van der Waals forces.

REFERENCES

1. S.P. McGlynn, T. Azumi, and M. Kinoshita, *Molecular Spectroscopy of the Triplet State,* Prentice-Hall, Englewood Cliffs, New Jersey, 1969

2. R.F. Borkman and D.R. Kearns, J. Chem Phys 44, 945 (1966)

3. E.C. Lim, Chem Phys Letters 1, 28 (1967)

4. A. Filhol, J. Phys Chem 75, 2056 (1971)

5. M.K. Orloff, P.A. Mullen, and F.C. Rauch, J. Phys Chem 74, 2189 (1970)

6. W. Selig, Explosivstoffe 4, 76 (1967)

7. C. Michaud, H. Mern, G. Poulin, and S. Lepage, C.R. Acad Sci Ser C, 267, 652 (1968)

8. W. Selig, Explosivstoffe 8, 174 (1966)

9. W.E. Bachmann and J.C. Sheehan, J. Am. Chem Soc 71, 1842 (1949)

10. G.F. Wright, et al, Can. J. Research 27B, 218, 462, 469, 489, 503, 520 (1949)

11. C.S. Choi and E. Prince, Acta Cryst B28, 2857 (1972)

12. J.Stals, Aust J. Chem 22, 2505 (1969)

13. B. Suryanarayana, J. Autera, and R. Graybush, Mol Cryst 2, 373 (1967)

14. J. Stals, A.S. Buchanan, and C.G. Barraclough, Trans Faraday Soc 67, 1749 (1970)

15. C.S. Choi and H.P. Boutin, Acta Cryst B26, 1235 (1970)

16. E.G. McRae and M. Kasha, J. Chem Phys 28, 721 (1958)

17. E.C. Lim and S.K. Chakrabarti, Mol Phys 13, 293 (1967)

18. B. Stevens, Spectrochim Acta 18, 439 (1962)

19. R.S. Mulliken and W.B. Person, in *Physical Chemistry, an Advanced Treatise,* Vol III, D. Henderson, ed, Academic Press, New York, 1969

20. R.S. Becker, *Theory and Interpretation of Fluorescence and Phosphorescence,* Wiley Interscience, New York (1969) p. 210

21. H. Beens and A. Weller, in *Molecular Luminescence,* E.C. Lim, ed, Benjamin, New York (1969)

22. C.A. Parker and C.G. Hatchard, Trans Faraday Soc 59, 284 (1963)

23. A.N. Terenin and V.L. Ermolaev, Dokl Akad Nauk SSSR 85, 547 (1952)

24. N. Hirota and C.A. Hutchison, Jr, J. Chem Phys 42, 2869 (1965)

25. J. Stals, C.G. Barraclough and A.S. Buchanan, Trans Faraday Soc 65, 904 (1969)

26. J.E. Mapes, private communication

27. J. Stals, Trans Faraday Soc 67, 1739 (1969)

28. D. Downs, private communication

29. J.N. Maycock, V.R. Pai-Verneker, and W. Lochte, Phys Stat Sol 35, 849 (1969)

30. C. Djerassi, H. Wolf, and E. Bunnenberg, J. Am. Chem Soc (London) 1965, p. 5002

31. I.B. Berlman in *Handbook of Fluorescence Spectra of Aromatic Molecules,* Academic Press, New York (1971)

32. D.P. Craig and S.H. Walmsley in *Excitons in Molecular Crystals,* W.A. Benjamin, Inc., New York (1968) p. 161

33. H. Leonhart and A. Weller, Ber Bunsenges, Physik Chemie 67, 791 (1963)

34. M. Blais, private communication

35. W.E. Bachmann and J.C. Sheehan, J. Am. Chem Soc 71, 1842 (1949)

36. G.F. Wright, et al, Can. J. Research 27B, 218, 462, 469, 489, 503, 520 (1949)

37. W.A. Schroeder, et al, Anal Chem 23, 1740 (1951)

38. R.N. Jones and G.D. Thorn, Can. J. Research 27B, 828 (1949)

39. L. Lang in *Absorption Spectroscopy in the Ultraviolet and Visible Region,* Vol VI, Academic Press, Inc., New York (1965)

40. M. Kasha, Radiation Research 20, 55 (1963)

41. S. Basu and J.H. Greist, J. Chimie Physique 59, 407 (1963)

42. P.L. Marinkas, unpublished

43. M.D. Cohen and Z. Ludmer, Chem Comm 1969, p. 1172

44. W. Helfrich and F.R. Lipsett, J. Chem Phys 43, 4368 (1965)

45. J. Stals, Doctoral Thesis, University of Melbourne, Melbourne, Australia, January 1970

46. F. Urbach, Phys Rev 92, 1324 (1953)

47. D.L. Dexter and R.S. Knox in *Excitons,* Interscience Tracts on Physics and Astronomy, No. 25, p. 125

48. S.J. Strickler and R.A. Berg, J. Chem Phys 37, 814 (1962)